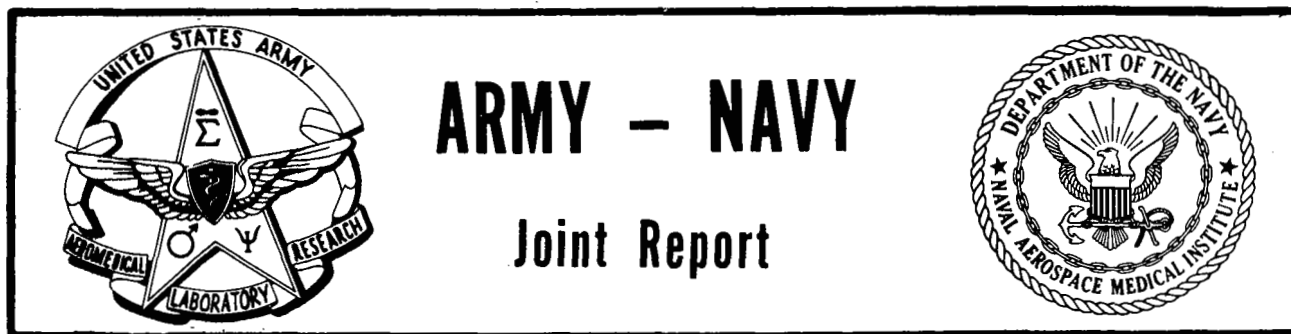


NAMI-1094

USAARL  
Serial No. 70-7

SAMPLE HELICOPTER FLIGHT MOTION DATA  
FOR VESTIBULAR REFERENCE

W. Carroll Hixson and Jorma I. Niven



U. S. ARMY AEROMEDICAL RESEARCH LABORATORY  
NAVAL AEROSPACE MEDICAL INSTITUTE

November 1969

This document has been approved for public release and sale; its distribution is unlimited.

This document has been approved for public release and sale;  
its distribution is unlimited.

SAMPLE HELICOPTER FLIGHT MOTION DATA  
FOR VESTIBULAR REFERENCE

W. Carroll Hixson and Jorma I. Niven

Bureau of Medicine and Surgery  
MF12.524.005-5016B

U. S. Army Aeromedical Research Laboratory

Approved by

Ashton Graybiel, M. D.  
Head, Research Department

Released by

Captain M. D. Courtney, MC USN  
Commanding Officer

26 November 1969

NAVAL AEROSPACE MEDICAL INSTITUTE  
NAVAL AEROSPACE MEDICAL CENTER  
PENSACOLA, FLORIDA 32512

## SUMMARY PAGE

### THE PROBLEM

The lack of man-referenced flight motion data to describe the vestibular-significant flight forces encountered in Army helicopter operations.

### FINDINGS

Presentation of low-frequency triaxial linear acceleration and triaxial angular velocity flight data collected on a noninterference basis in seven different military helicopters performing various flight maneuvers.

### ACKNOWLEDGEMENTS

The authors wish to acknowledge both Mr. C. A. Lowery of the Medical Electronics Branch for the considerable field trip effort involved in the collection of the flight data and Mr. R. C. Barrett of the Photographic Services Section for his contribution to the reproduction of these data in report form. In addition, the authors wish to thank the many personnel at the U. S. Army Aviation Test Board who made possible the collection of the AH-1G "Huey Cobra" flight data.

-----

The findings in this report are not to be construed as an official Department of the Army position, unless so designated by other authorized documents.

Trade names of materials or products of commercial or nongovernment organizations are cited only where essential to precision in describing research procedures or evaluation of results. Their use does not constitute official endorsement or approval of the use of such commercial hardware or software.

## INTRODUCTION

In the flight environment man's visual perception of his own motion and attitude in space is dependent upon the availability of some external geographical landmark or feature for measurement reference. When these features are clearly observable without illusory artifact, he encounters little difficulty in maintaining control of his spatial orientation. In the absence of such visual references man's vestibular system and related nonvisual sensory processes become the predominant source of information for spatial perception. The information provided by these nonvisual receptors is, in the normal terrestrial environment, usually quite adequate to define the instantaneous spatial orientation of an individual. In the airborne environment, however, these sensing mechanisms are exposed to flight forces and torques which can produce illusory sensations of spatial orientation that are in complete conflict with the actual motion or attitude of the aircraft. In all cases the exact form of these erroneous responses is dependent upon the magnitude and anatomical orientation of the resultant flight accelerations. Before the vestibular field can make applied or operational contributions to the understanding of the form, magnitude, and direction of these illusory responses, measurement data which describe quantitatively the resultant linear and angular motion characteristics of a given aircraft environment must be made available. However, as has been stressed in an earlier report (3) on a kinematics based nomenclature for vestibular stimuli, the measurement data must be referenced to selected morphological coordinates of man, rather than to the coordinates of some vehicle or device, if directly relevant descriptions of motion stimuli are to be achieved.

In this light, we initiated a measurement program on a joint basis with the U. S. Army Aeromedical Research Laboratory (USAARL) to collect such man-referenced flight motion data in the military helicopter environment. To implement this program a low-cost instrumentation system was developed that could be installed on a noninterference basis in various U. S. Army helicopters and used to record the low-frequency triaxial linear accelerations and triaxial angular velocities encountered in flight. The technical considerations, measurement philosophy, and design criteria involved in the development of this system have been described in two previous reports (1, 2). Upon completion and flight test of the system it was installed in a variety of currently operational military helicopters, and flight data were collected during selected aircraft tactical maneuvers as well as routine flight operations. In addition, a second instrumentation package of identical form was constructed, flight tested, and delivered to USAARL to facilitate their continuing assimilation of such flight data. This summary report presents sample excerpts of the triaxial motion data collected to date in seven different helicopter types. It is the intent that these preliminary data will provide vestibular workers an introductory familiarization with the general characteristics of selected helicopter force environments.

## INSTRUMENTATION

The instrumentation system developed for the collection of the helicopter flight motion data presented in this report contains all transducers, signal-conditioning amplifiers, recording equipment, and battery power sources necessary to measure and record the following: the triaxial linear accelerations of the aircraft occurring along its roll, pitch, and yaw axes; the triaxial angular velocities occurring about the same axes; and descriptive voice annotation of the in-progress flight maneuver or operation. Since the project priority was such that all flight data had to be collected on a complete noninterference basis, the system was designed so as to be self-contained and self-powered in a single package, thus requiring no structural modifications, instrumentation services, or power demands from the aircraft itself.

To facilitate interpretation of the flight records presented in the report a brief review of the technical characteristics of the main elements of the system follows: The linear acceleration measurement data were collected by means of three hermetically sealed, gas-damped, linear accelerometers (Humphrey Inc., Model LA45) with potentiometer readout. Each transducer had a full-scale range of  $\pm 2g$ , a natural frequency of 22 cps, and a damping ratio between 0.6 and 0.7. The three angular velocity transducers were dc-operated, gimballess rate gyros (Humphrey Inc. Series RG-28), with potentiometer readout, a full-scale range of  $\pm 100$  deg/sec, a natural frequency of 25 cps, and a damping ratio of  $0.7 \pm 0.2$ . The output signals from these transducers were separately routed to six solid-state dc operational amplifiers (Philbreck Inc., Model P25C) which provided the gain and impedance matching necessary to drive the system recorder. A 6 db per octave RC filter rolled off each of these amplifiers at 100 cps. In-flight storage of the motion data was by a 7-channel, magnetic tape instrumentation recorder (Lockheed Electronics Co. Model 417D) utilizing the standard IRIG format on 1/2-inch tape. Using FM type record electronics and a tape speed of 7 1/2 ips, the frequency response of each recording channel extended from 0 to 2,500 cps. Voice annotation was on a separate edge track. The capacity of the system batteries was such that flight data could be collected continuously for intervals extending to 90 minutes. For this particular study the system was packaged in a near cubical configuration measuring approximately 16 inches on each side. A photograph of the package taken immediately before installation in an AH-1G "Huey Cobra" is shown in Figure 1.

## PROCEDURE

A photograph taken during the preflight checkout of the instrumentation recorder installation aboard an OH-6A "Cayuse" observation helicopter is shown in Figure 2. With the exception of the AH-1G "Huey Cobra" and the CH-54 "Flying Crane," the instrumentation system was hard mounted to the deck in the forward pilot compartment immediately adjacent to the pilot seat. In the AH-1G the system was installed in the forward copilot seat of the aircraft. The ventilated seat cushions and seat armor plates were removed and replaced by a 1/4-inch thick aluminum plate aligned with the horizontal reference plane of the aircraft. The base of the instrumentation package was then bolted directly to this plate. In the CH-54 the package was installed in the aft pilot



Figure 1. View of AH-1G "Huey Cobra" showing relative size of flight recorder system.

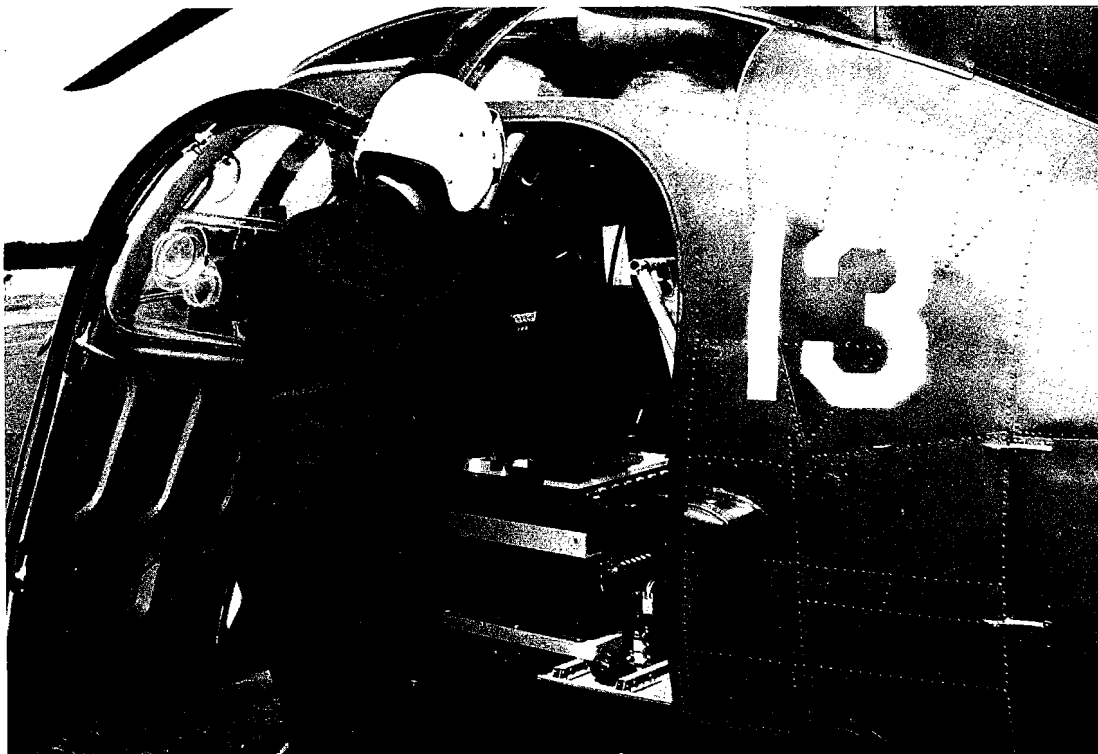


Figure 2. View of OH-6A "Cayuse" showing installation of flight recorder immediately behind pilot seat.

compartment at the request of the aircraft pilot. In all cases, the orthogonal  $x$ ,  $y$ , and  $z$  axes of sensitivity of the transducer assembly were aligned with the roll, pitch, and yaw axes, respectively, of the aircraft.

Upon completion of the installation in a given aircraft, the only request made to the pilot was that he fly a series of standard operational maneuvers he thought would be "typical" for the aircraft. Interestingly, almost without exception, the pilots said that they would fly maneuvers typical to "Stateside operations" but not typical to "Viet Nam operations." They would then explain that in many combat situations, they would perform evasive maneuvers involving high bank angles and turn rates that they would never repeat in a noncombat situation.

## RESULTS AND DISCUSSION

Selected excerpts from the in-flight magnetic tape recordings made aboard seven different helicopters are presented in Figures 3 through 62. The basic nomenclature (3) and the display format used for all these records are as follows: The top three measurement channels describe three mutually orthogonal components of the instantaneous resultant linear acceleration of the aircraft at the site of the transducer package; these components are identified as  $A_x$ ,  $A_y$ , and  $A_z$  where the  $x$ ,  $y$ , and  $z$  subscripts denote the roll, pitch, and yaw axes, respectively, of the aircraft. Accordingly,  $A_x$ ,  $A_y$ , and  $A_z$  describe the instantaneous linear acceleration of the aircraft in the fore-aft, port-starboard, and vertical directions, respectively. The bottom three measurement channels, identified as  $\omega_x$ ,  $\omega_y$ , and  $\omega_z$ , describe the instantaneous angular velocity of the aircraft in terms of its components acting about the same three axes. The direction or polarity conventions used to display these kinematically described linear acceleration and angular velocity components are summarized in Table I where the positive sense derives from  $+x$  being directed forward,  $+y$  leftward, and  $+z$  ceilingward. Time-base reference is established at the bottom of each record by means of 1-second timing pulses.

Magnitude reference for the six measurement channels is given by the calibration marks placed at the left of each display, along with the related plus and minus polarity conventions. For each linear acceleration channel the signal magnitude is expressed as a multiple of  $g = 32.174 \text{ ft/sec}^2$ . The center horizontal line of the  $A_z$  channel corresponds to a linear acceleration level of  $+1.0g$ , while the same center reference for the  $A_x$  and  $A_y$  channels corresponds to a  $0.0g$  level. This gives a more optimal display of the  $A_z$  data as a result of the  $1.0g$  contribution of gravitational action that, in most cases, is directed along the  $+z$  aircraft axis. It should be noted, however, that although the  $A_z$  baseline is displaced relative to the  $A_x$  and  $A_y$  channels, the same full-scale  $g$  range is used for all three channels. In the three angular velocity channels the measurement units are degrees/second, with all three channels having the same display sensitivity. The display sensitivity of each measurement channel is the same throughout all the flight records presented in the report.

Table I

## Summary of Nomenclature and Recording Conventions Used to Describe Flight Data

| Linear Acceleration Units: Multiples of $g = 32.174 \text{ ft/sec}^2$ |                    |                         |
|---|--------------------|-------------------------|
| Data Symbol   | Stimulus Direction | Galvanometer Deflection |
| $+A_x$  | forward            | up                      |
| $-A_x$  | backward           | down                    |
| $+A_y$  | leftward           | up                      |
| $-A_y$  | rightward          | down                    |
| $+A_z$  | headward           | up                      |
| $-A_z$  | footward           | down                    |
| Angular Velocity Units: degrees/second                                |                    |                         |
| $+\omega_x$   | roll right         | up                      |
| $-\omega_x$   | roll left          | down                    |
| $+\omega_y$   | pitch down         | up                      |
| $-\omega_y$   | pitch up           | down                    |
| $+\omega_z$   | yaw left           | up                      |
| $-\omega_z$   | yaw right          | down                    |

A last point pertinent to the interpretation of these flight records involves the upper frequency limit of the displayed data. Though the direct-writing galvanometer recorder (Sanborn Company, Model 358) used to write-out the data had a frequency response extending from 0 to approximately 100 cps, the 20-to 25-cps natural frequency rating of the transducer elements of the system serves as the key upper roll-off frequency. Since the vestibular investigator is concerned primarily with low-frequency stimuli, the bulk of the flight data was passed through a low-pass, single section RC filter with a 5-cps corner frequency before being displayed on the galvanometer recorder. This type of filtered display is typified by Figure 3 which represents the flight motion data collected aboard the high performance AH-1G "Huey Cobra" attack aircraft during an actual rocket-firing run. In this maneuver, the aircraft entered a dive midway in the record following a gradual left turn, was aligned in roll and yaw attitude relative to the fixed target, the side-mounted rockets were fired, and the helicopter then went into a 1.75-g pull-up accompanied by a gradual right turn.

Introduction of this 0 to 5 cps filter removes the bulk of the low-frequency vibrations superimposed on the linear acceleration and angular velocity signals describing the basic motion profile of the aircraft in three-dimensional space. However, since low-frequency vibration, torsional as well as translational, cannot be neglected relative to performance degradation, sample flight motion data are also presented without this 5-cps low pass filter. The unfiltered form of display is typified by Figure 4 which describes the identical AH-1G rocket-firing run shown in Figure 3. The same form of filtered and unfiltered comparison is achieved in Figures 5 and 6 for a AH-1G machine-gun run, with Figure 6 illustrating the significant rise occurring in vibration level during the pull of positive  $g$  along the  $z$  axis. The same applies for Figures 7 and 8 during a left turn and Figures 9 and 10 during a right turn.

The third and last form of display involves a change in the time-base of the displayed data and is represented by Figures 11 and 12. Here, the triaxial linear and angular motion data are displayed without filtering on an expanded time-base so as to illustrate the basic waveform of the low-frequency vibration of the aircraft along and about the three reference axes. The Figure 11 data were collected during liftoff of the AH-1G while the Figure 12 data were obtained during straight and level flight at 150 knots. Differences in the frequency spectrum presented by these two flight conditions are readily apparent.

Similar flight data collected aboard a UH-1B "Huey" gunship are presented in Figures 13 through 24. Representative motion profiles include several 7.62-mm "mini-gun" target runs, two left and right evasive turn maneuvers, and a cyclic climb-out. Expanded time-scale recordings made during straight and level flight and during a climbing right turn of the UH-1B are also included. The remainder of the data is of similar self-explanatory form, with motion profiles collected aboard a UH-1D "Huey" troop ship presented in Figures 25 through 28; an OH-6A "Cayuse" observation helicopter in Figures 29 through 38; a CH-54 "Flying Crane" in Figures 39 through 46; a CH-47A "Chinook" in Figures 47 through 56; and a UH-2B "Seasprite" in Figures 57 through 62.

The separate presentation of these linear and angular motion flight data in simple triaxial component form follows the emphasis we have placed previously (3) on the need for quantitative man-referenced identifications of the basic motion parameters of vestibular-significant force environments. Since the  $x$ ,  $y$ , and  $z$  measurement reference axes are, for all practical purposes, in parallel alignment with the front-back, left-right, and head-foot axes, respectively, of the conventionally seated pilot in these aircraft, the vestibular investigator will find no difficulty in relating these motion parameters to the classical forms of vestibular stimulation. Some obvious further data-processing techniques that can be applied without difficulty to these basic data include computer computation of the magnitude and anatomical direction of the resultant linear and angular vectors, the same for the magnitude and direction of that component of the resultant acting in each of the three cardinal head planes, and various frequency spectrum analyses. However, when first beginning the investigation of the stimulus-response relationships occurring in a complex force environment, it has been our experience that greatest immediate insight to the problem will be offered by analysis of the individual components of the resultant.

## REFERENCES

1. Hixson, W. C., A triaxial accelerometer module for vestibular application. NAMI-1040. USAARU Serial No. 68-9. Pensacola, Fla.: Naval Aerospace Medical Institute, and U. S. Army Aeromedical Research Unit, 1968.
2. Hixson, W. C., and Niven, J. I., Instrumentation for measurement of vestibular-significant forces in helicopters. NAMI-1043. USAARU Serial No. 68-10. Pensacola, Fla.: Naval Aerospace Medical Institute, and U. S. Army Aeromedical Research Unit, 1968.
3. Hixson, W. C., Niven, J. I., and Correia, M. H., Kinematics nomenclature for physiological accelerations: With special reference to vestibular applications. Monograph 14. Pensacola, Fla.: Naval Aerospace Medical Institute, 1966.

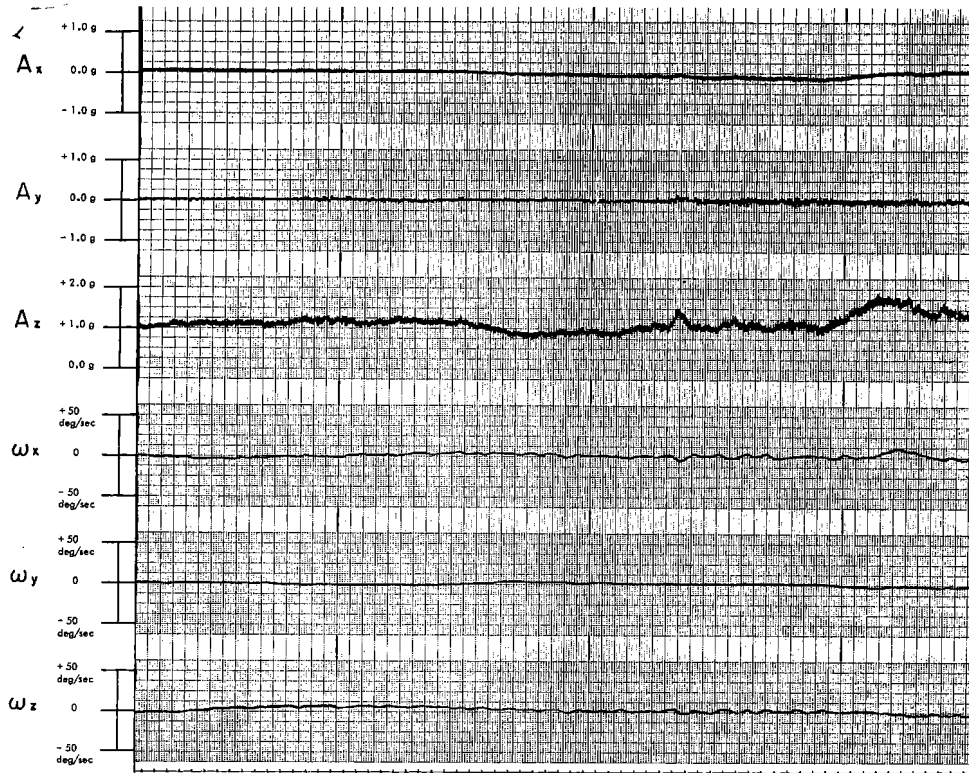


Figure 3. Flight data collected aboard an AH-1G "Huey Cobra" attack helicopter during a 150-knot rocket-firing run. The raw flight-data signals were routed through a 0-5 cps low-pass filter. See text for details.

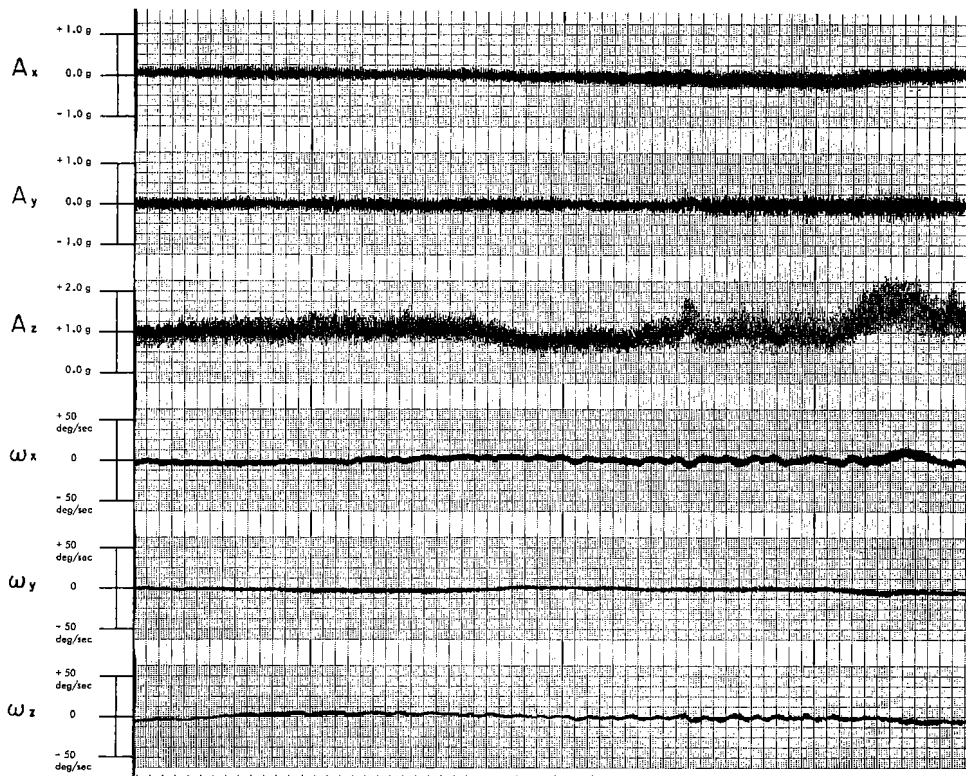


Figure 4. AH-1G flight data: Same as Figure 3 except not filtered.

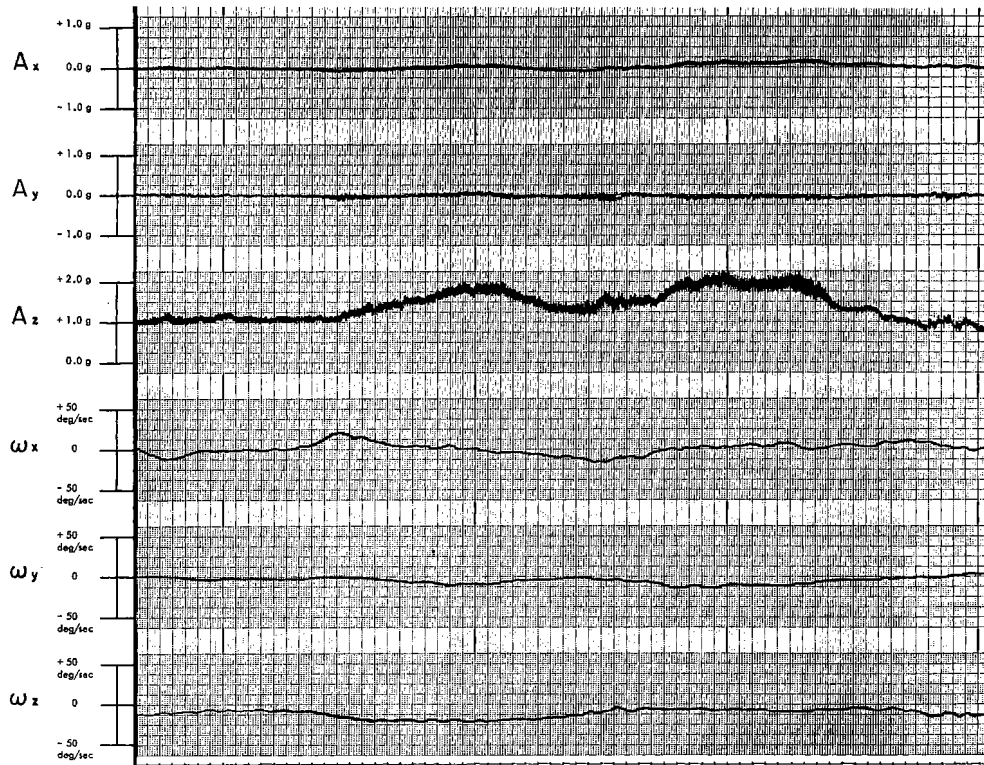


Figure 5. AH-1G flight data collected during a 150-knot machine-gun-firing run: 0 to 5 cps filter.

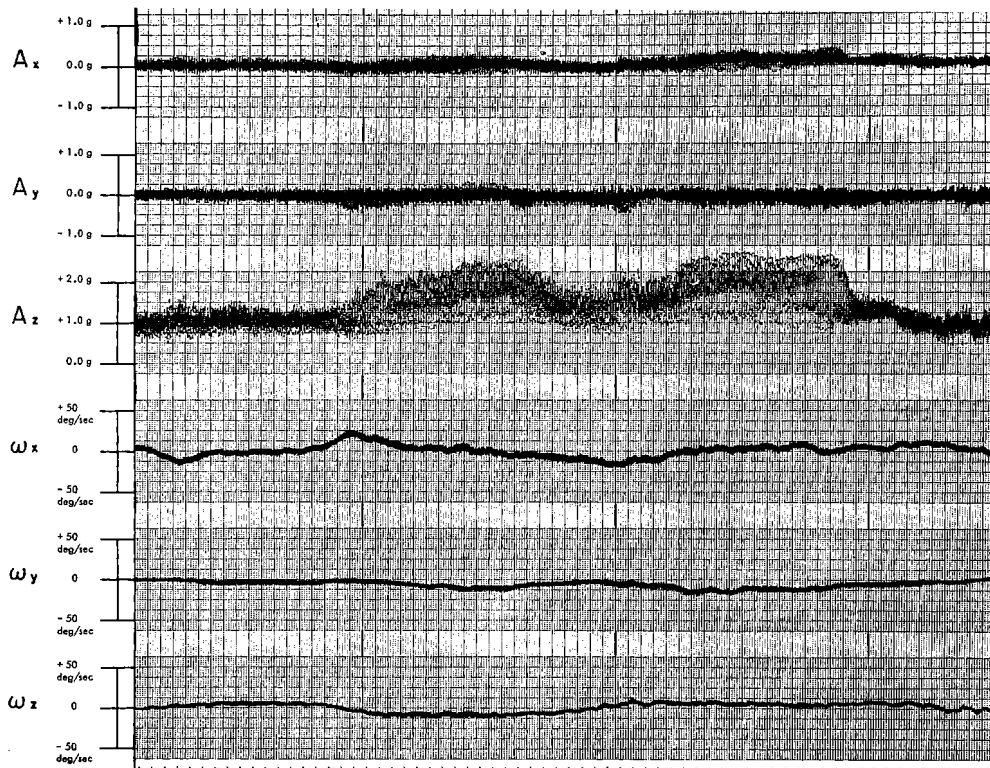


Figure 6. AH-1G flight data: Same as Figure 5 except not filtered.

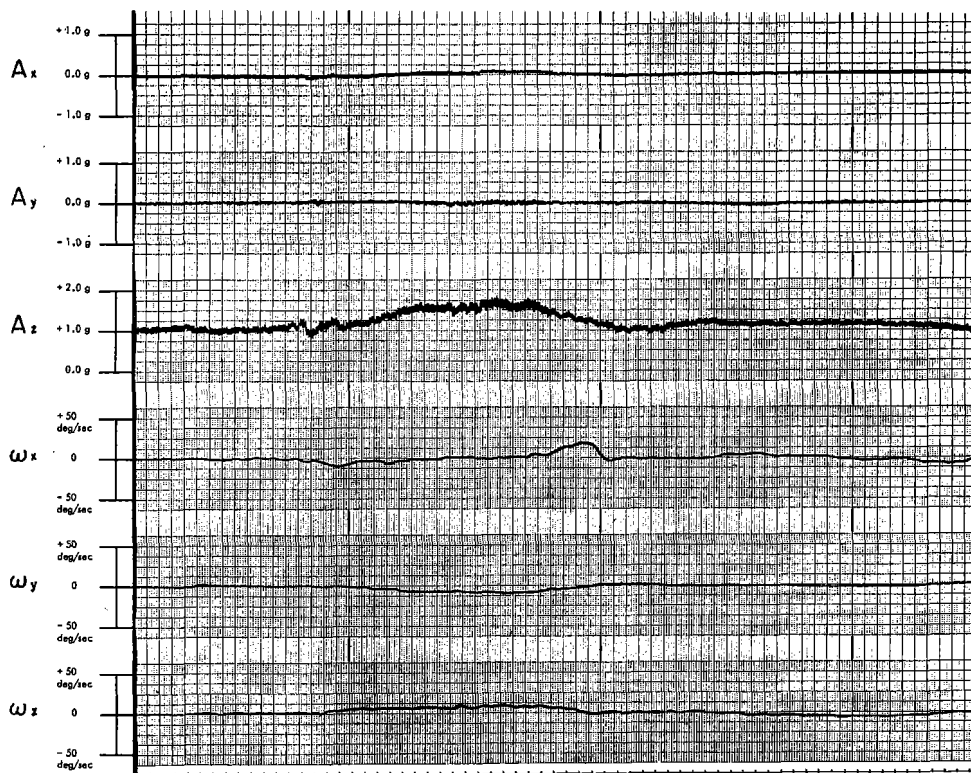


Figure 7. AH-1G flight data collected during a left turn maneuver: 0 to 5 cps filter.

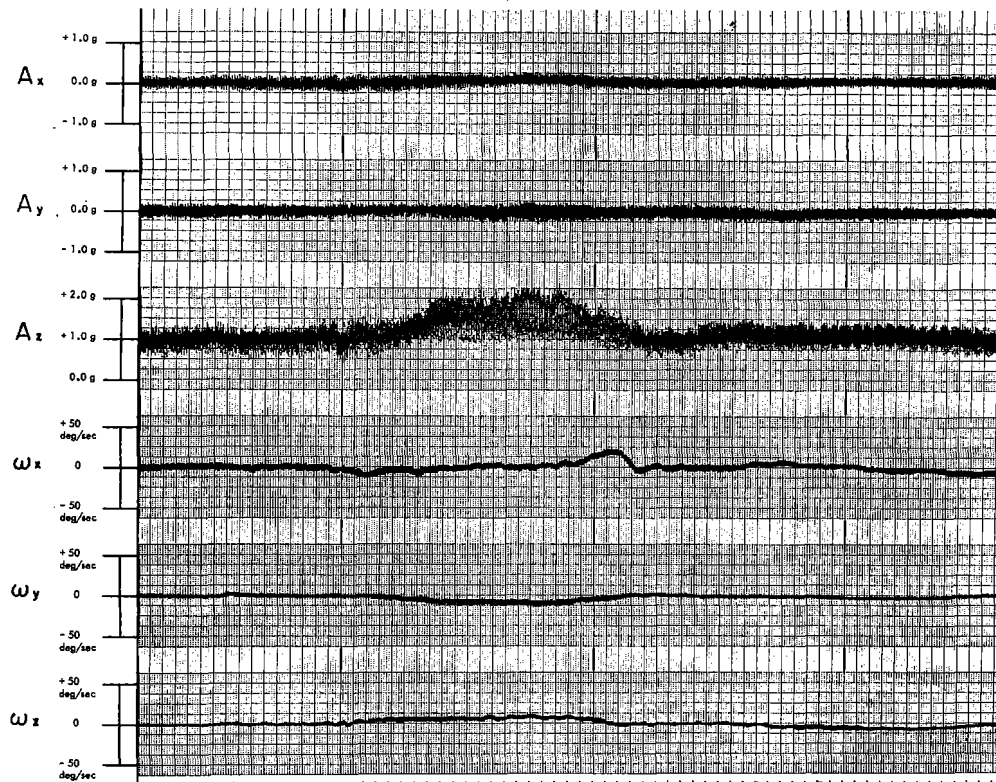


Figure 8. AH-1G flight data: Same as Figure 7 except not filtered.

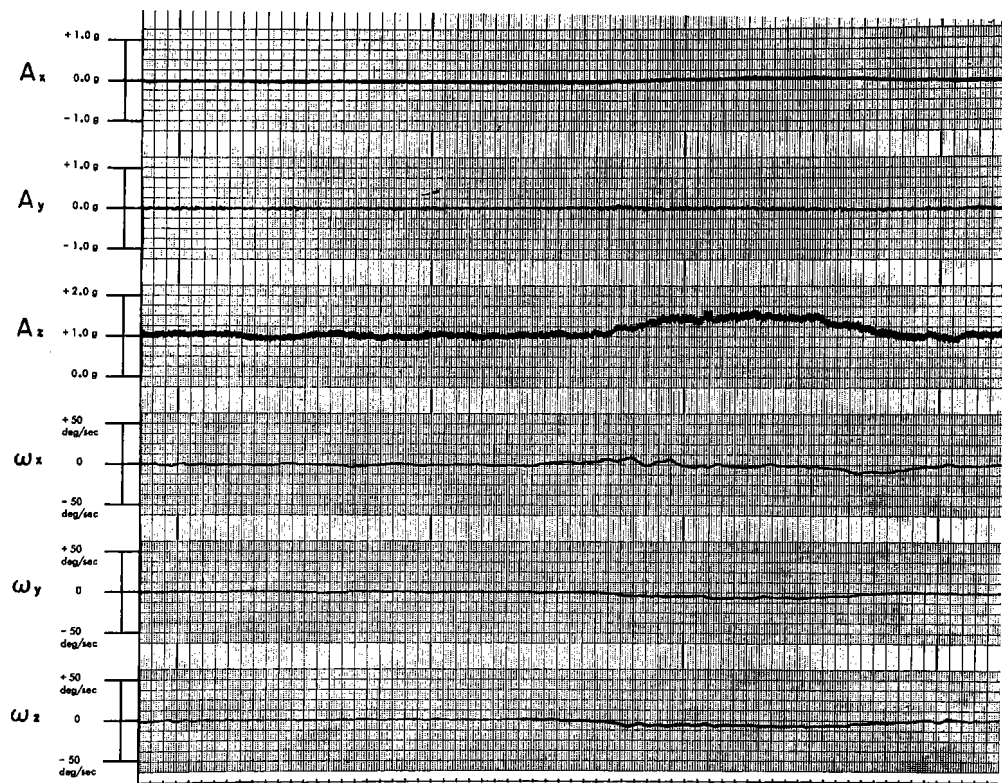


Figure 9. AH-1G flight data collected during a right turn maneuver: 0 to 5 cps filter.

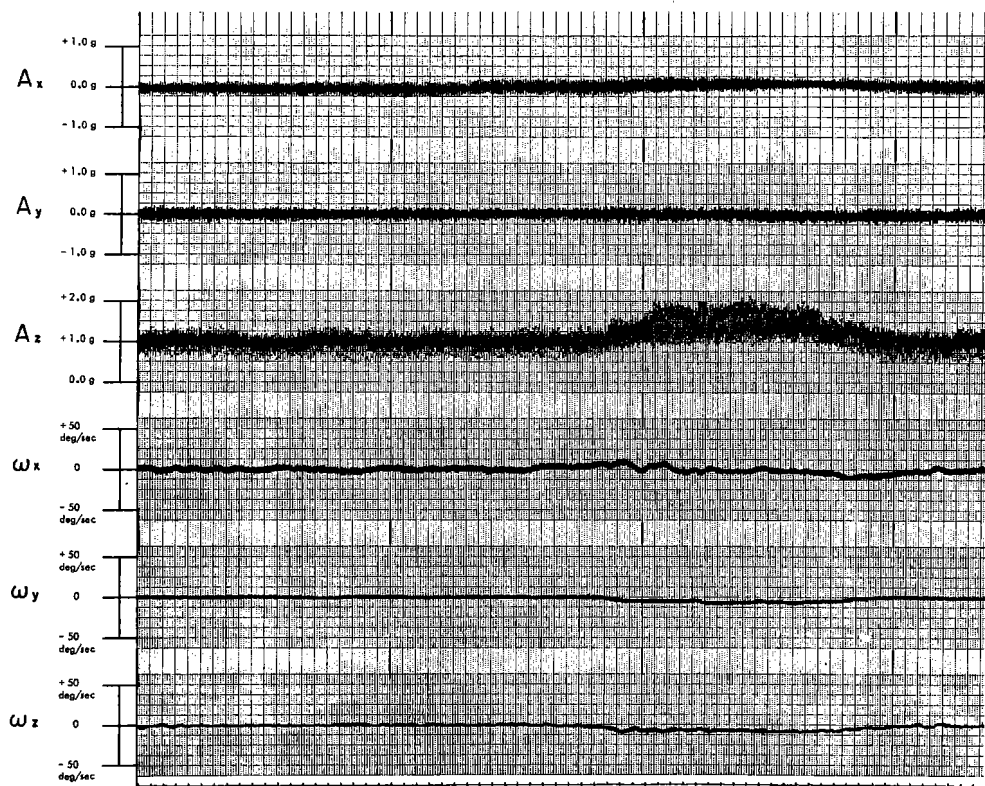


Figure 10. AH-1G flight data: Same as Figure 9 except not filtered.

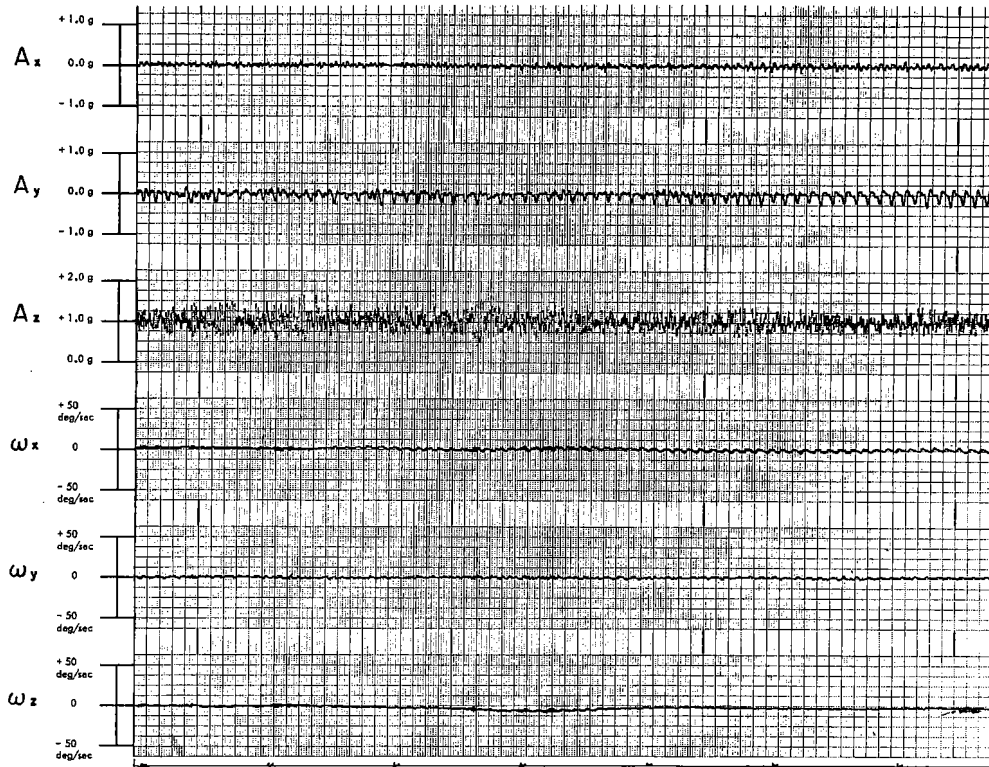


Figure 11. AH-1G flight data: Expanded time-base (note 1-second timing markers) recording made during liftoff. Data not filtered.

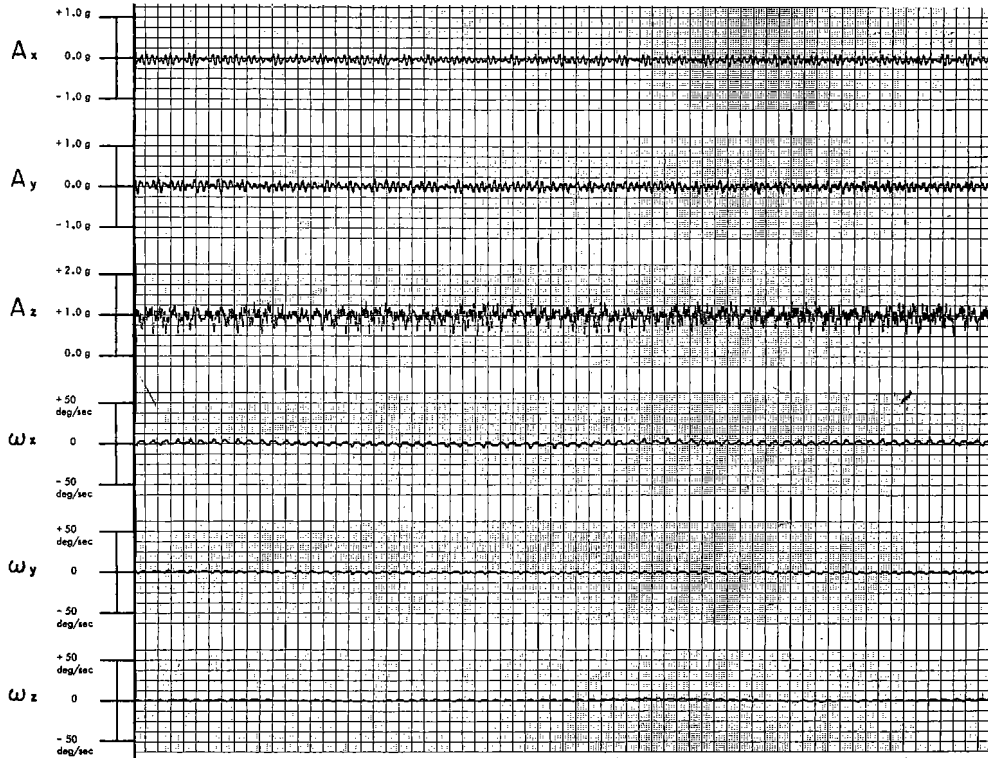


Figure 12. AH-1G flight data: Expanded time-base recording made during straight and level flight at 150 knots. Data not filtered.

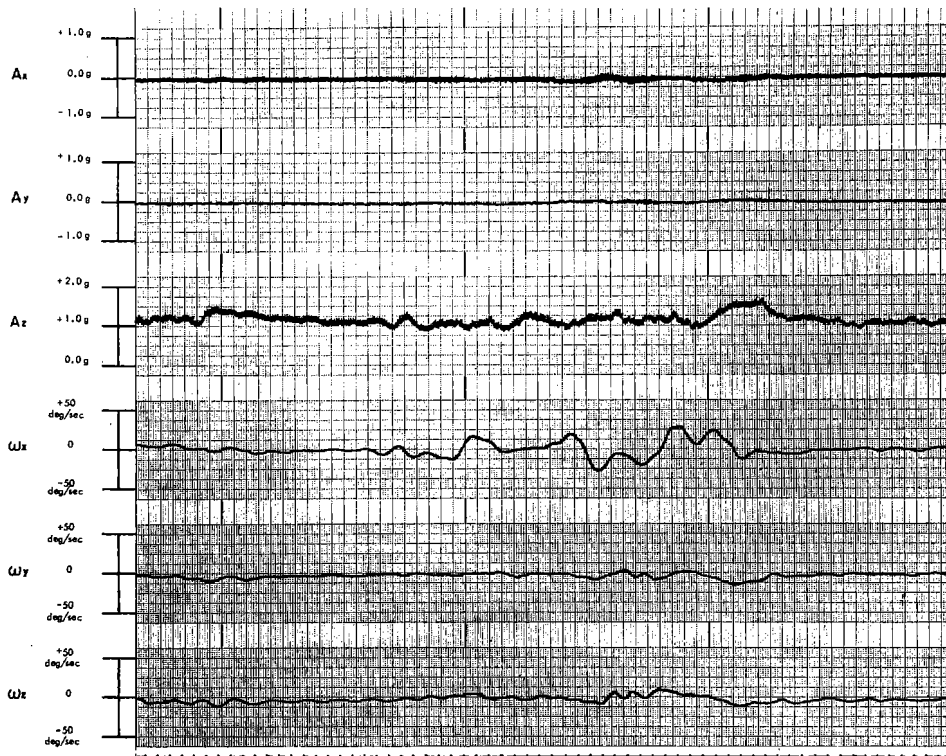


Figure 13. UH-1B "Huey" flight data collected during a 7.62-mm minigun-firing-run made at 90 knots: 0 to 5 cps filter.

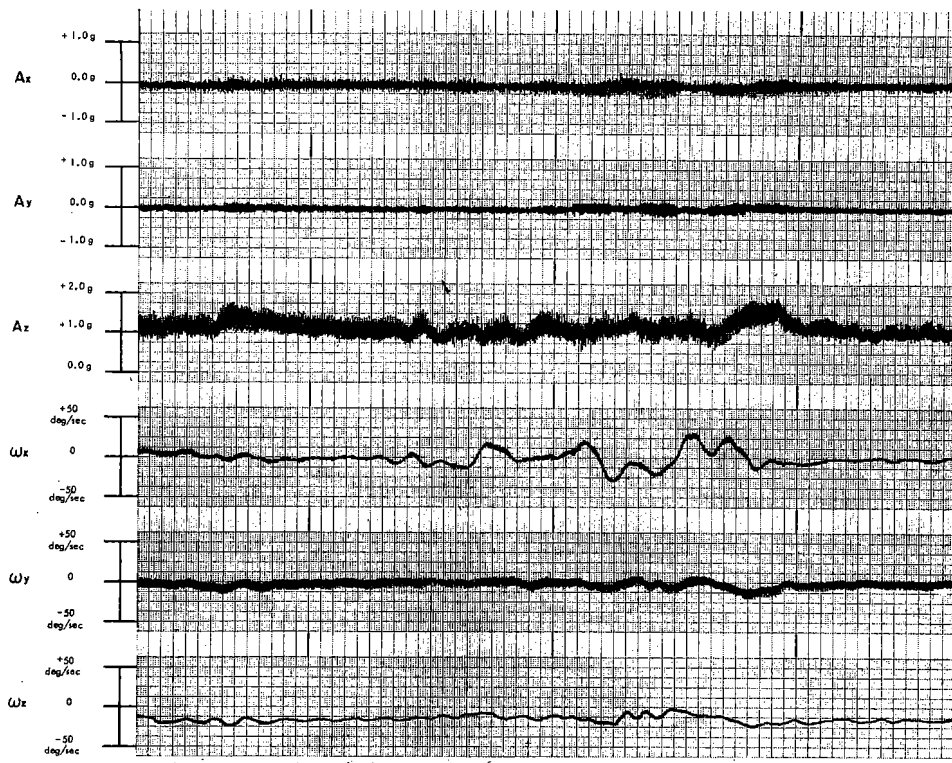


Figure 14. UH-1B flight data: Same as Figure 13 except not filtered.

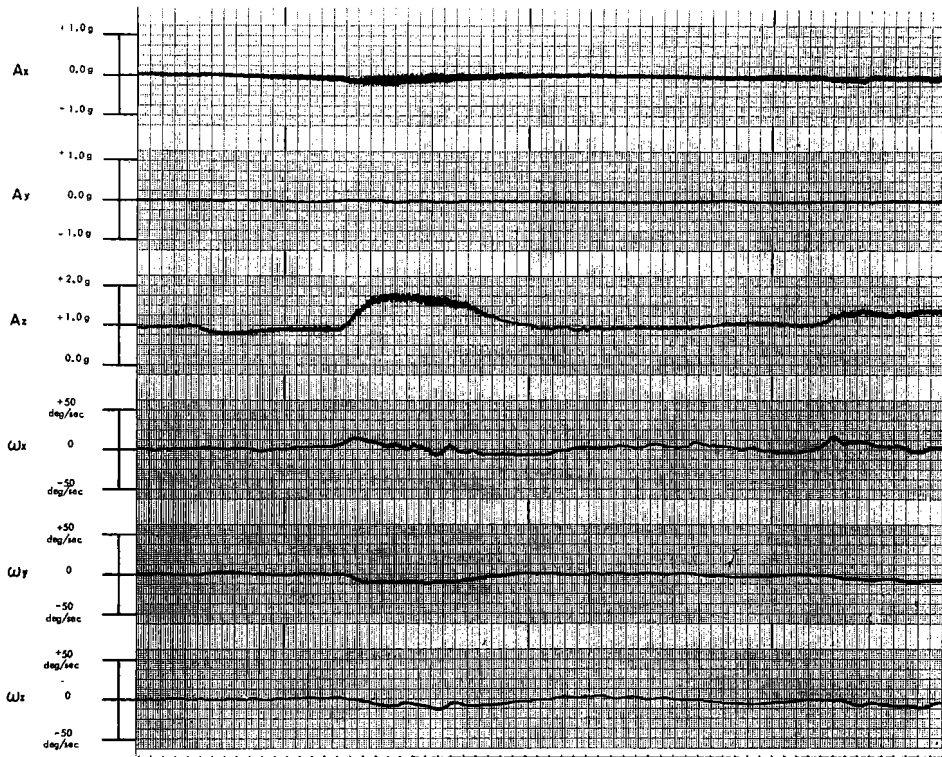


Figure 15. UH-1B flight data collected during a 90-knot diving target approach maneuver: 0 to 5 cps filter.

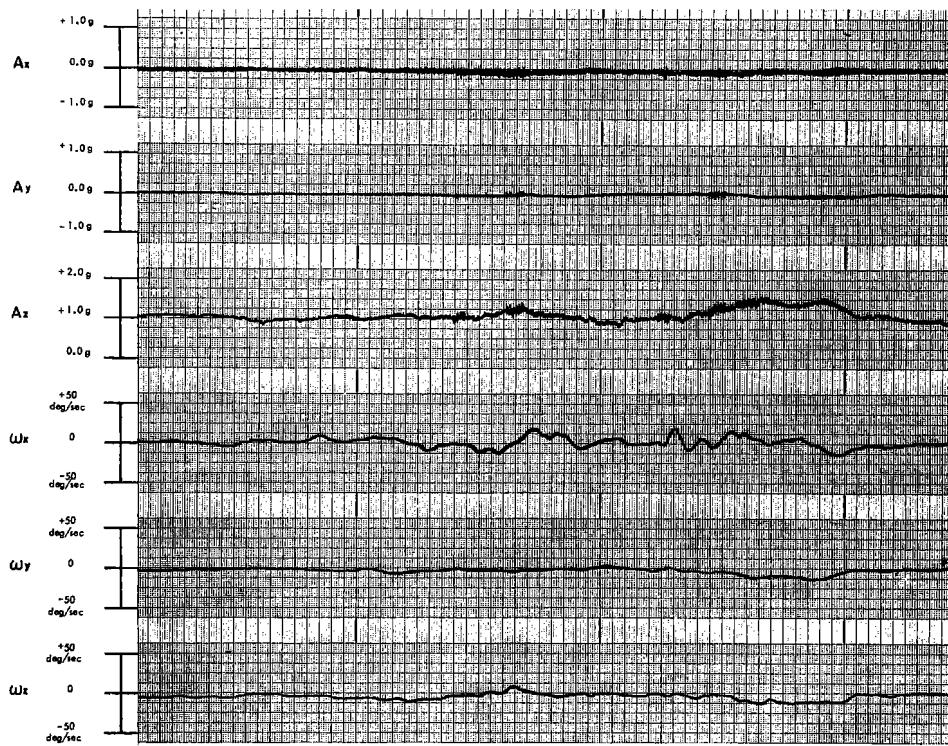


Figure 16. UH-1B flight data collected during a 40-mm grenade-firing run involving successive left and right banks as approaching the target: 0 to 5 cps filter.

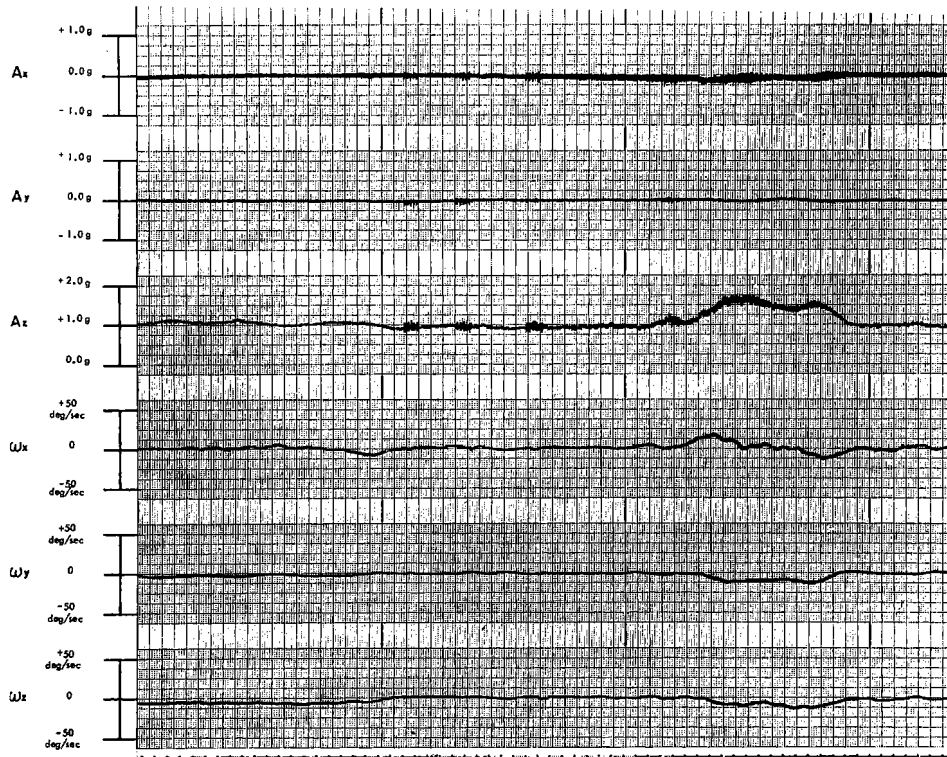


Figure 17. UH-1B flight data collected in a second 40-mm grenade-firing run: 0 to 5 cps filter.

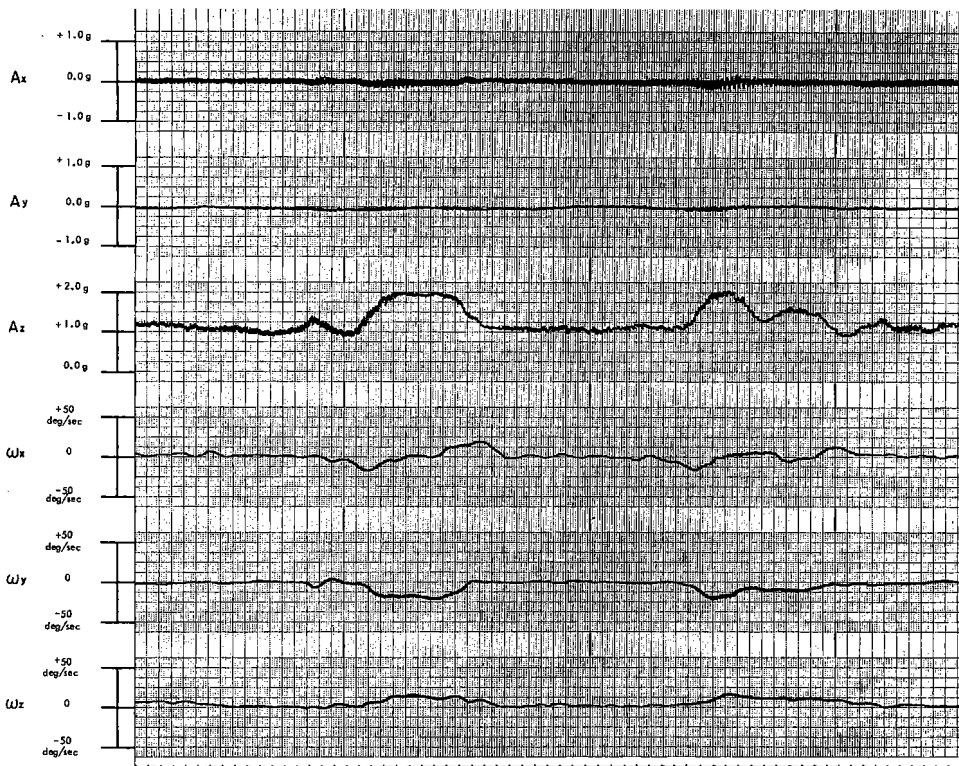


Figure 18. UH-1B flight data collected during a typical left turn used for evasive action: 0 to 5 cps filter.

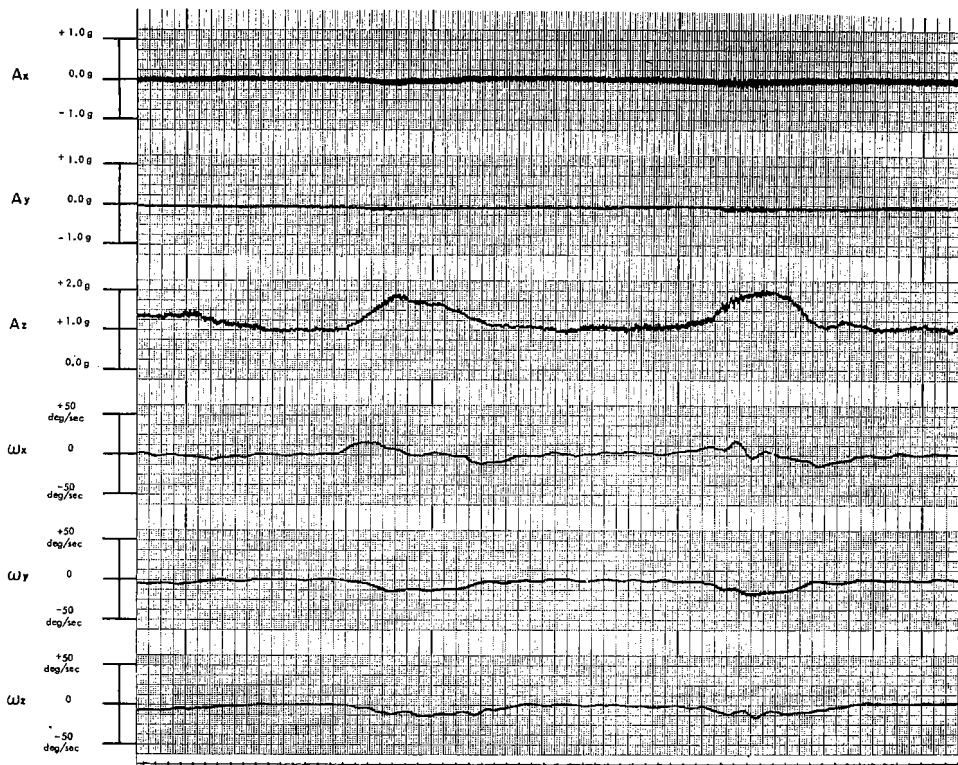


Figure 19. UH-1B flight data collected during a typical right turn used for evasive action: 0 to 5 cps filter.

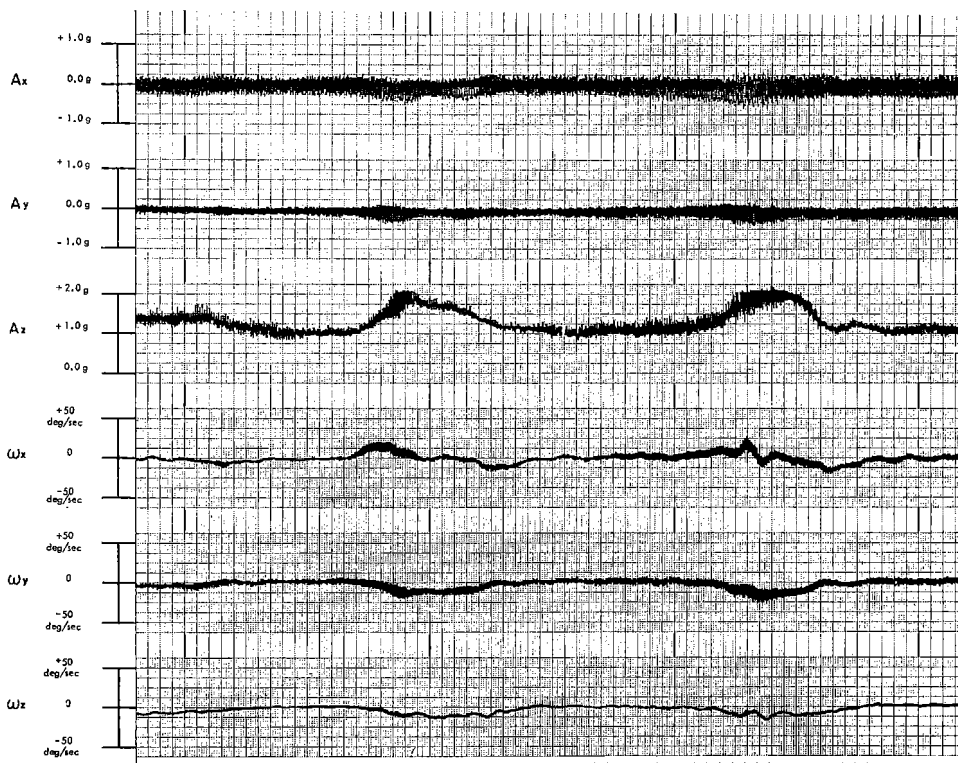


Figure 20. UH-1B flight data: Same as Figure 19 except not filtered.

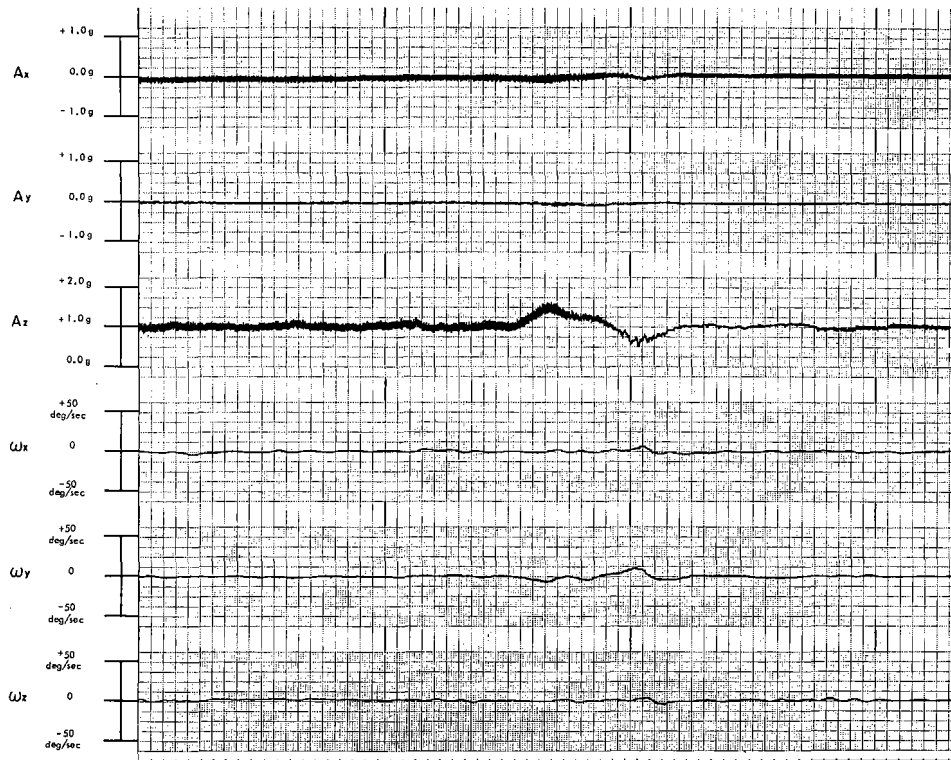


Figure 21. UH-1B flight data collected during a cyclic climbout: 0 to 5 cps filter.

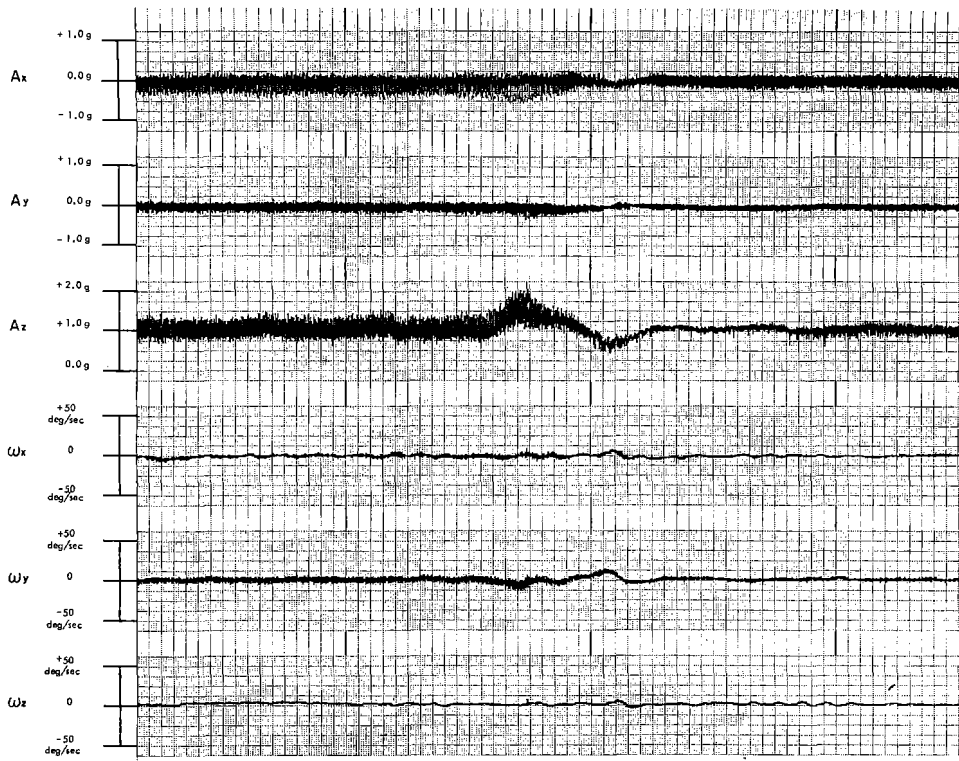


Figure 22. UH-1B flight data: Same as Figure 21 except not filtered.

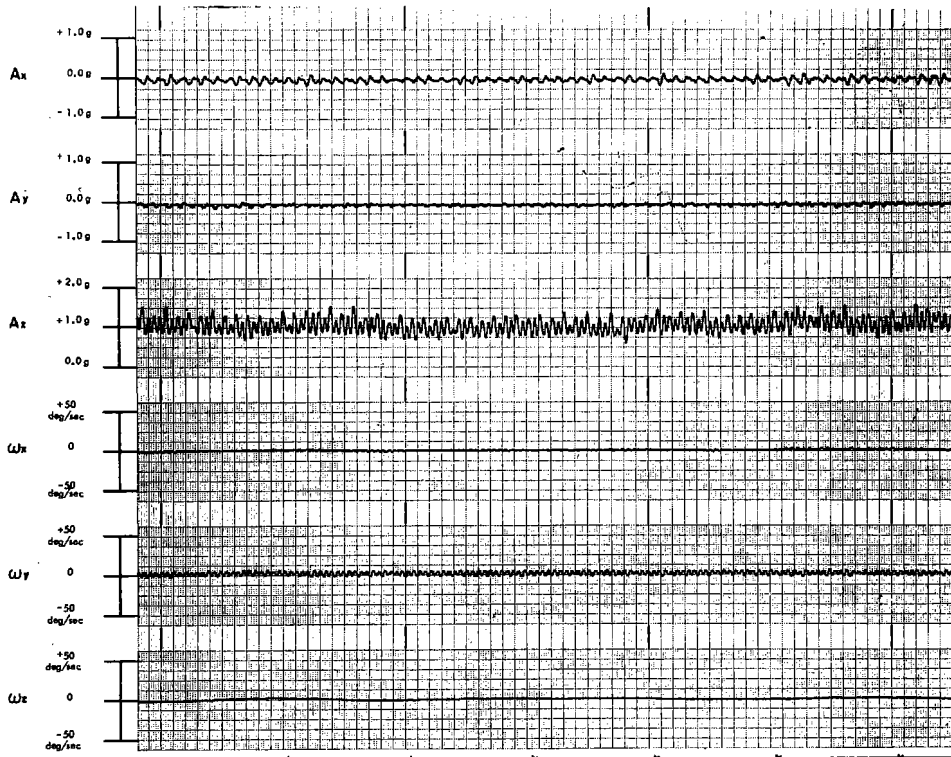


Figure 23. UH-1B flight data: Expanded time-base recording made during straight and level flight at 90 knots. Data not filtered.

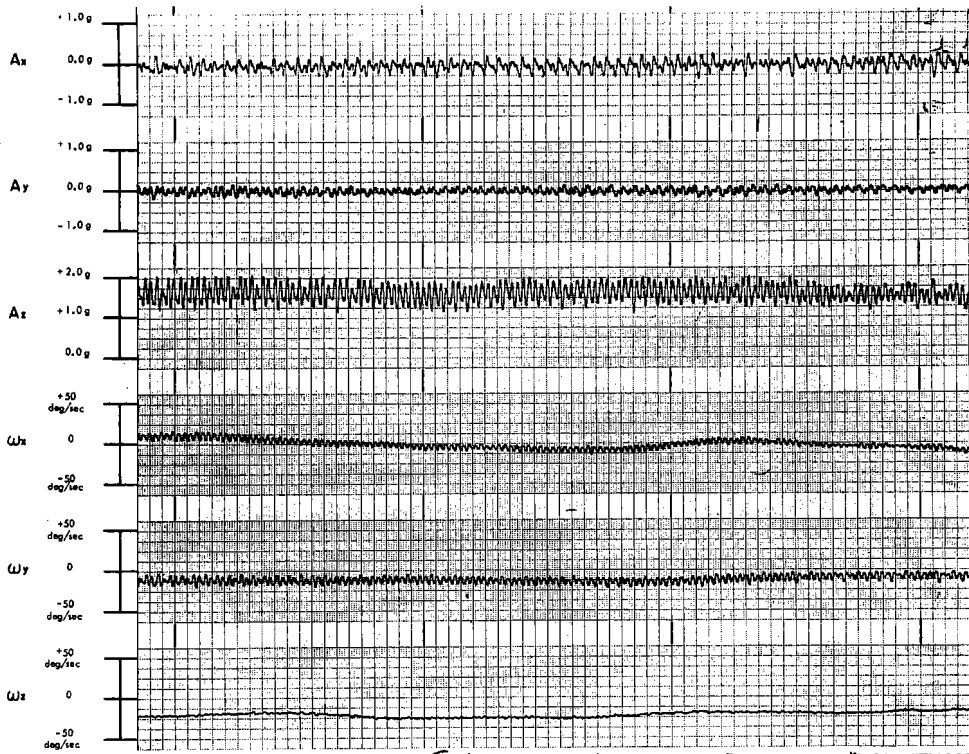


Figure 24. UH-1B flight data: Expanded time-base recording made during a climbing right turn. Data not filtered.

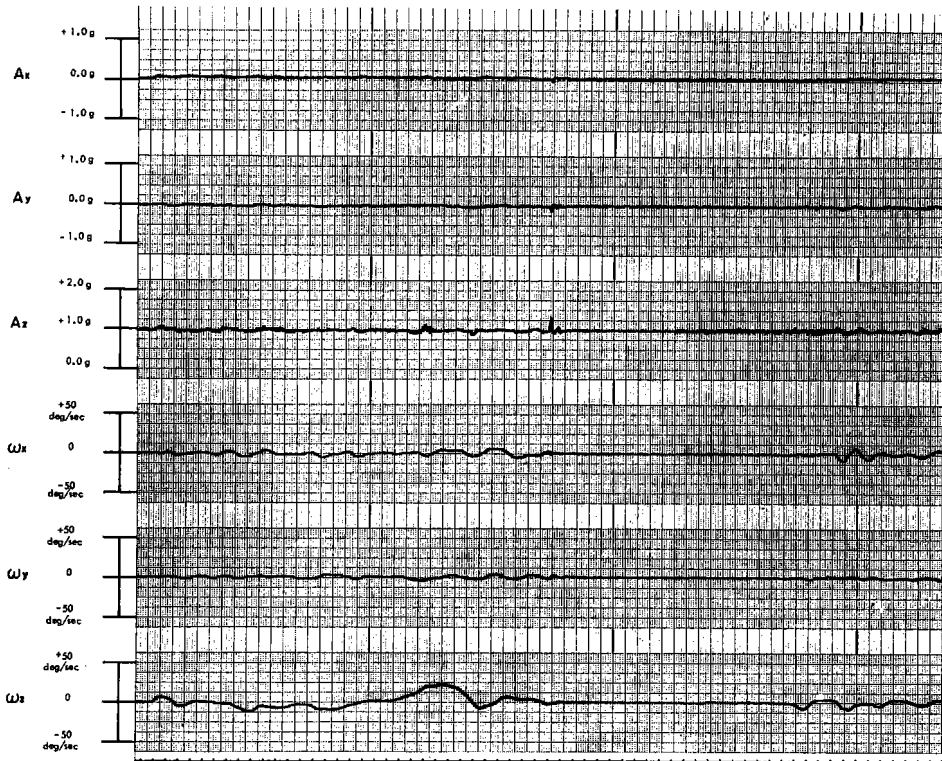


Figure 25. UH-1D "Huey" flight data collected during a practice formation landing involving a brief touch-down for off-loading troops: 0 to 5 cps filter.

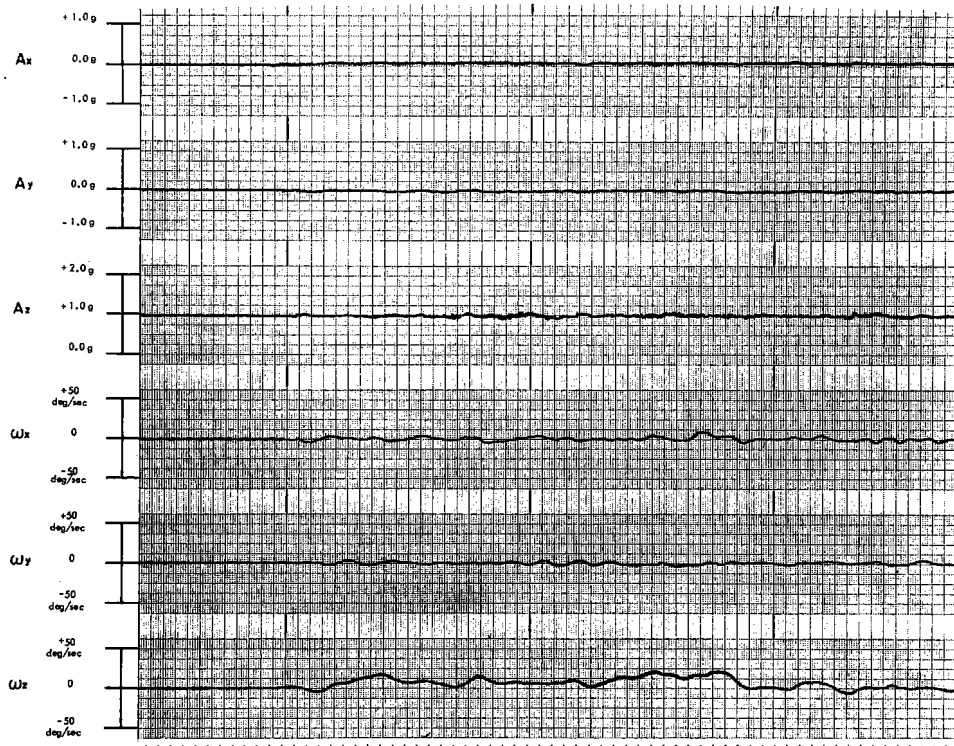


Figure 26. UH-1D flight data collected during a formation liftoff into hover followed by an on-the-spot left turn: 0 to 5 cps filter.

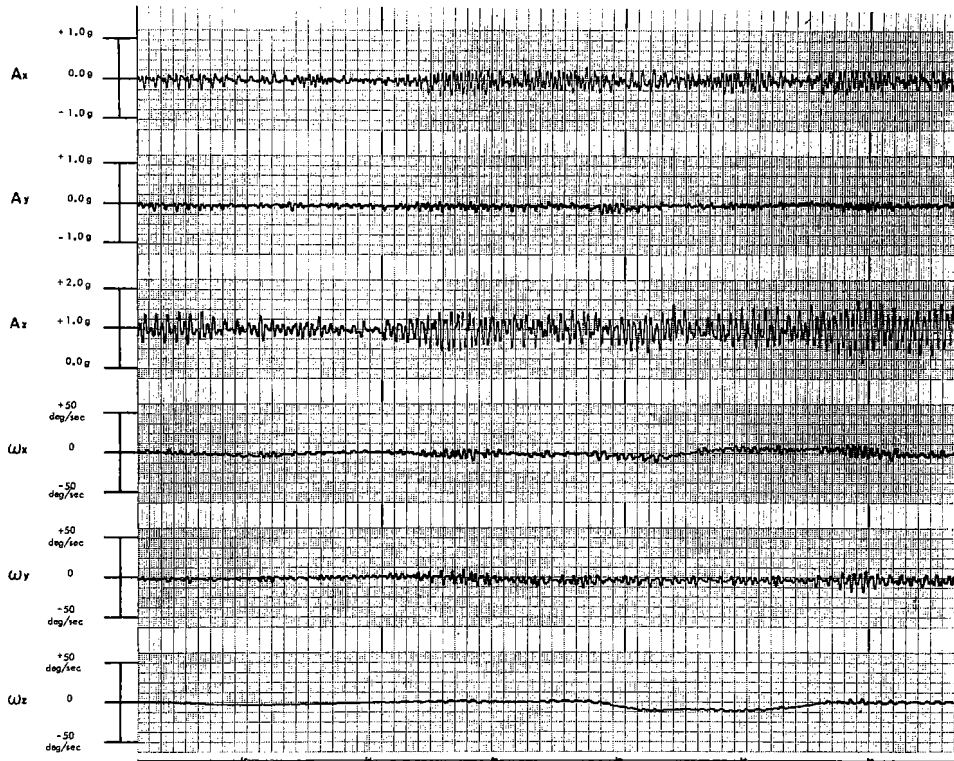


Figure 27. UH-1D flight data: Expanded time-base recording made during a landing approach. Data not filtered.

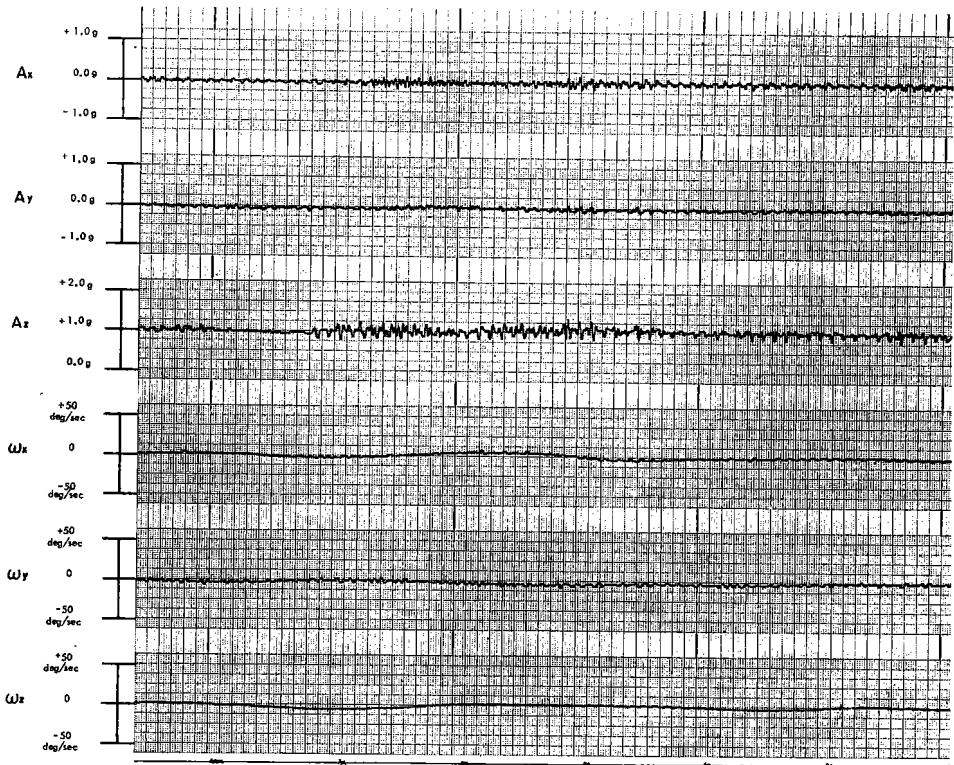


Figure 28. UH-1D flight data: Expanded time-base recording made during takeoff. Data not filtered.

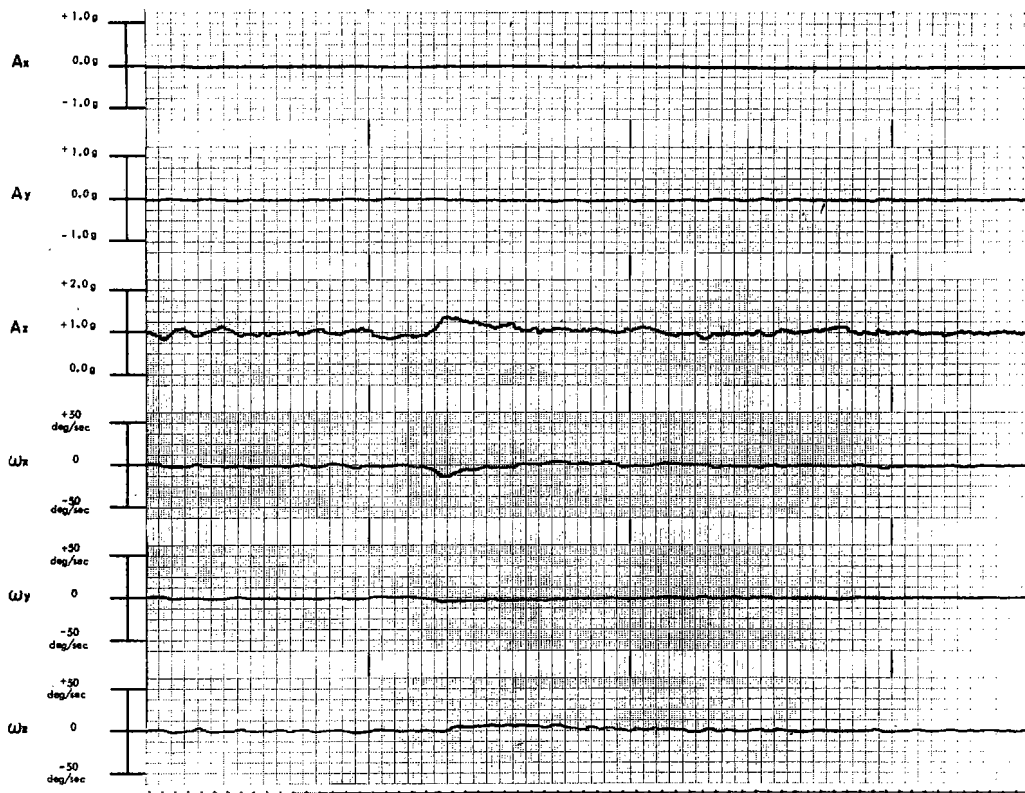


Figure 29. OH-6A "Cayuse" flight data collected during a descending left turn: 0 to 5 cps filter.

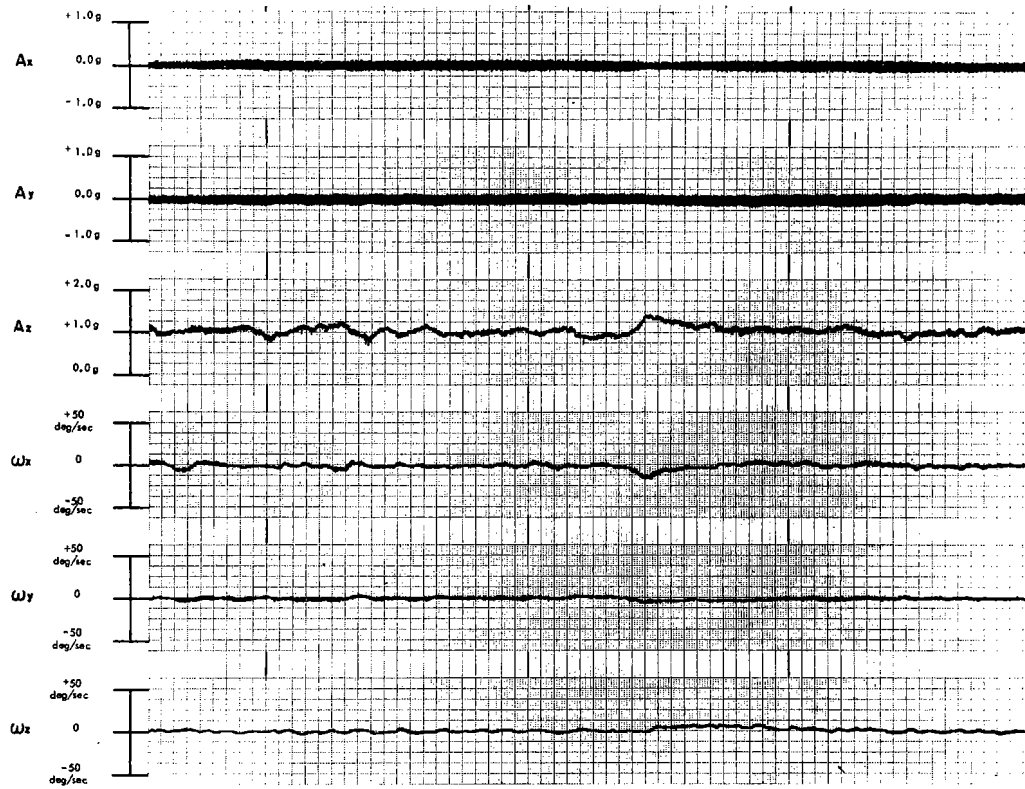


Figure 30. OH-6A flight data: Same as Figure 29 except not filtered.

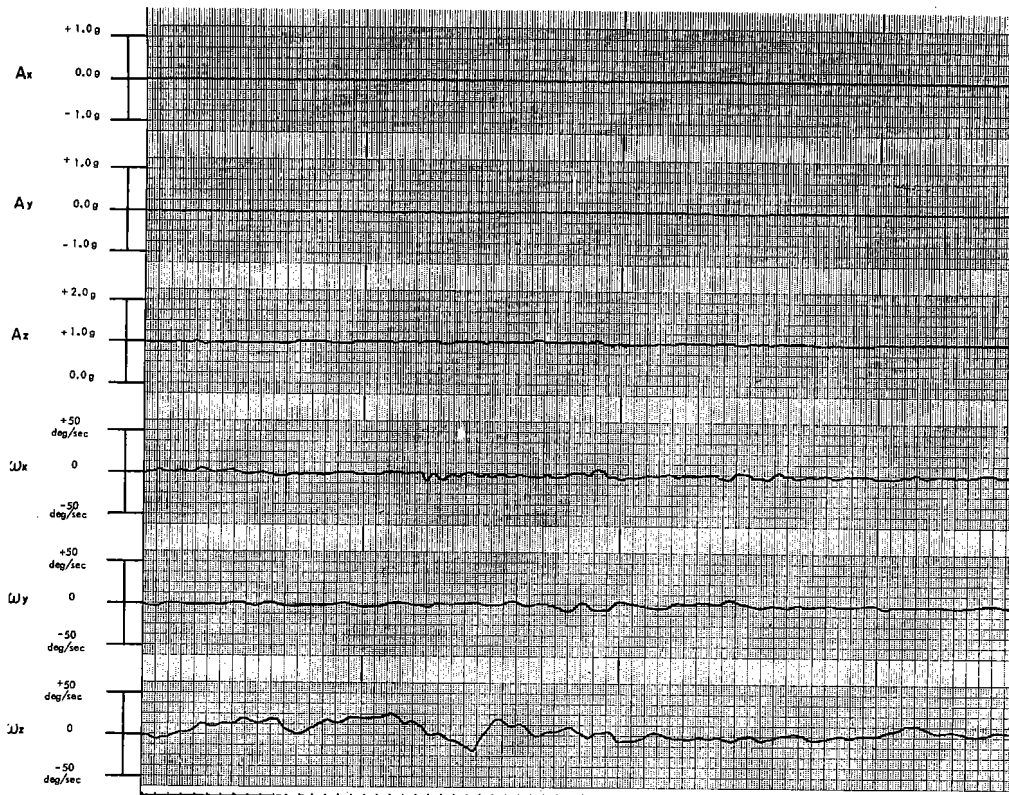


Figure 31. OH-6A flight data collected during a typical hovering turn: 0 to 5 cps filter.

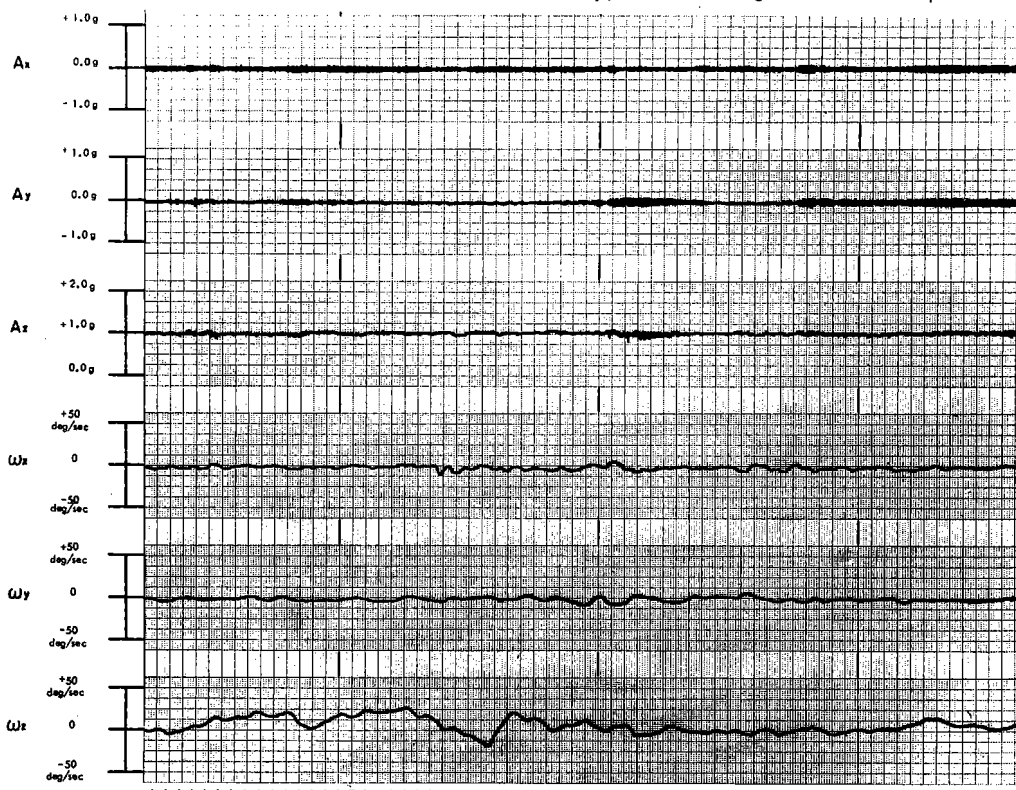


Figure 32. OH-6A flight data: Same as Figure 31 except not filtered.

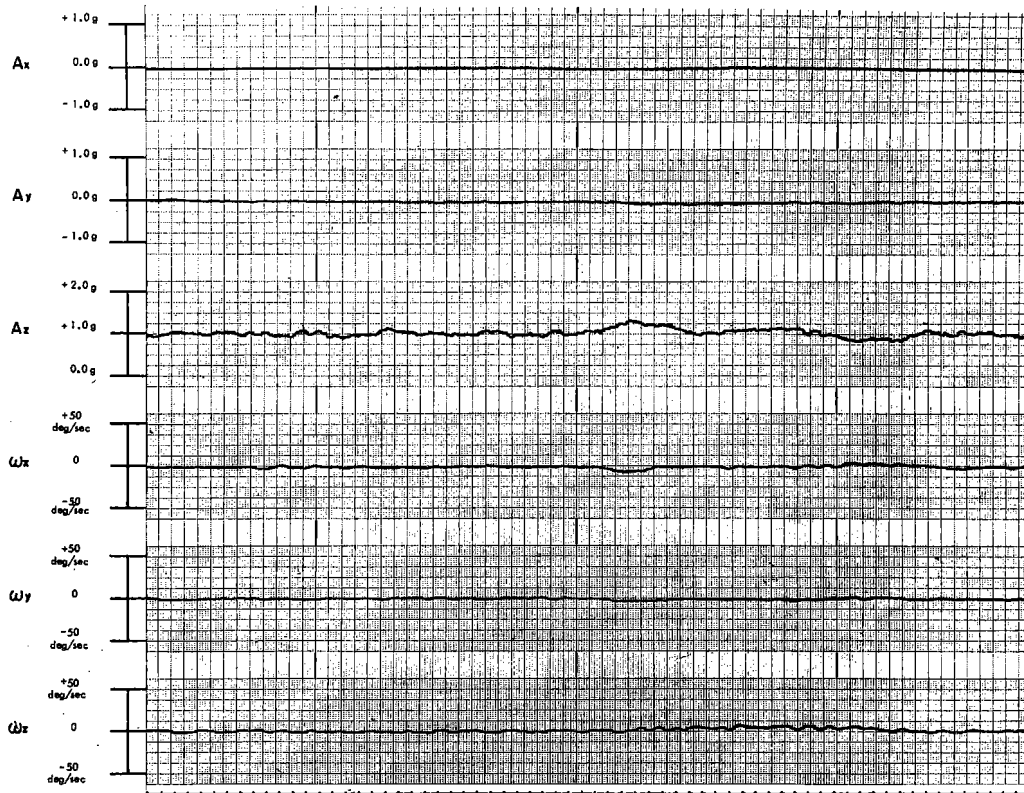


Figure 33. OH-6A flight data collected during a 90-knot climbing left turn: 0 to 5 cps filter.

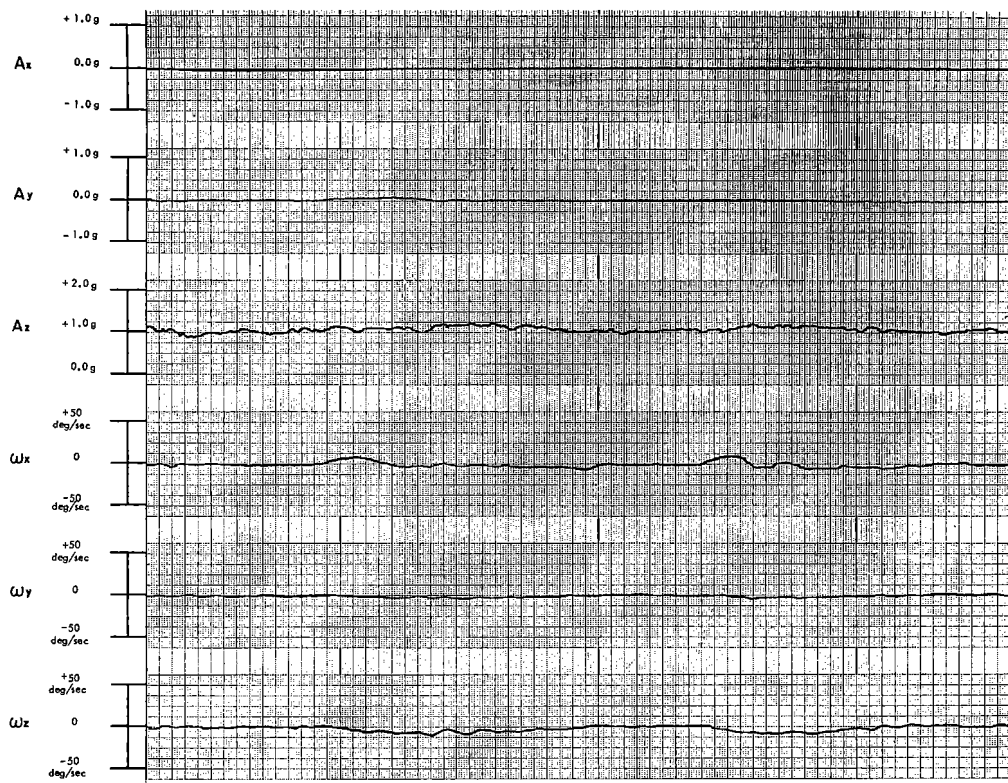


Figure 34. OH-6A flight data collected during a descending right turn: 0 to 5 cps filter.

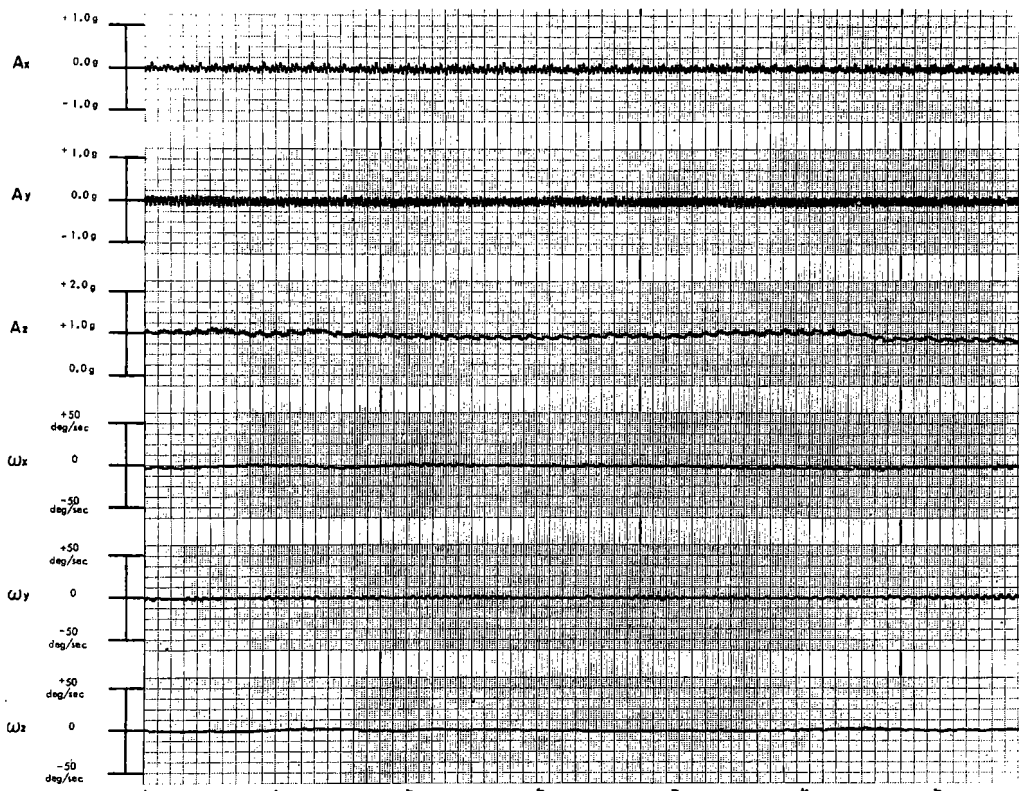


Figure 35. OH-6A flight data: Expanded time-base recording made during straight and level flight at 95 knots. Data not filtered.

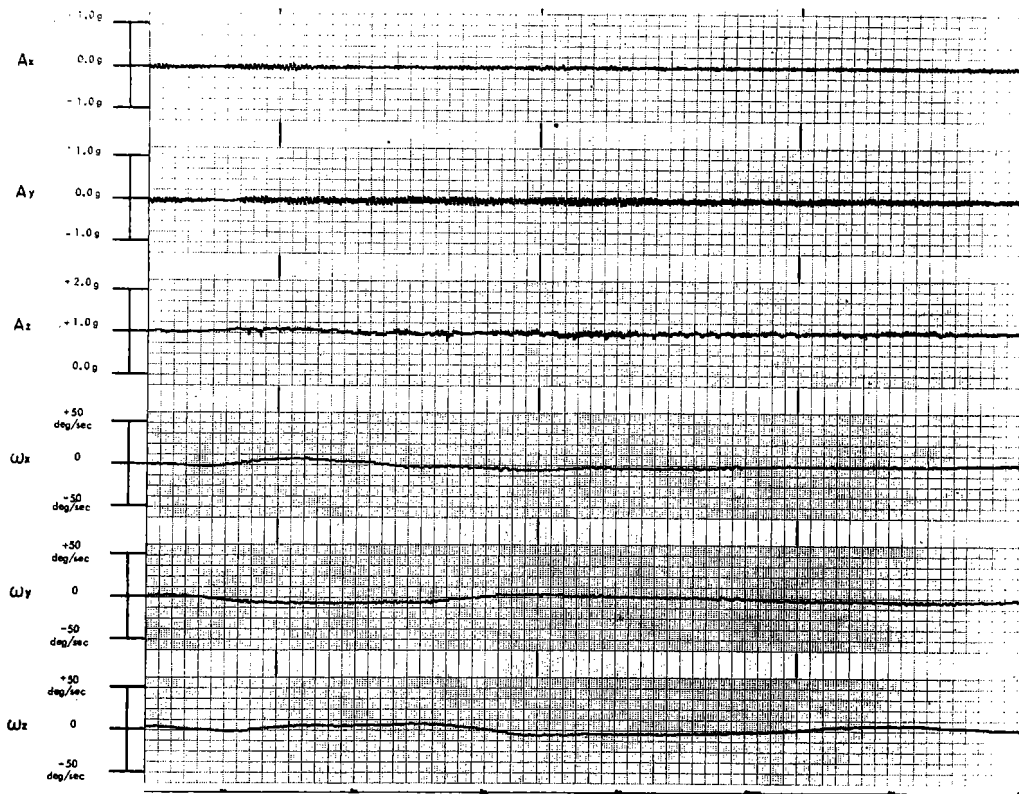


Figure 36. OH-6A flight data: Expanded time-base recording made while hovering. Data not filtered.

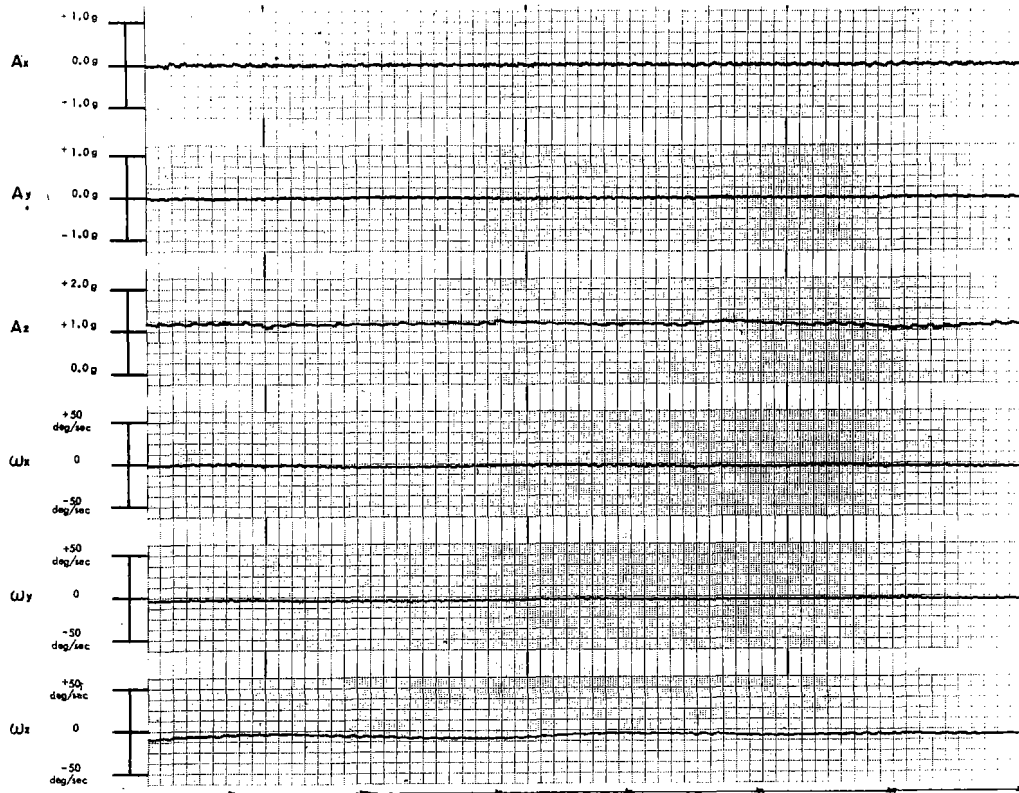


Figure 37. OH-6A flight data: Expanded time-base recording made during a right turn. Data not filtered.

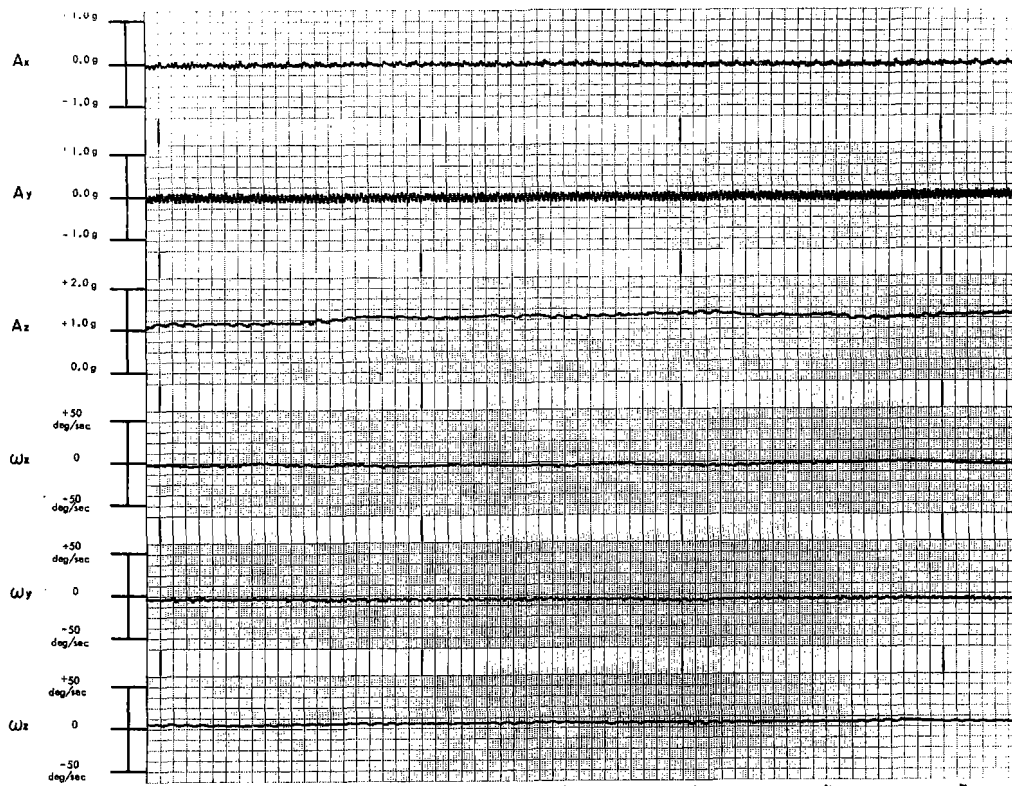


Figure 38. OH-6A flight data: Expanded time-base recording made during a left turn. Data not filtered.

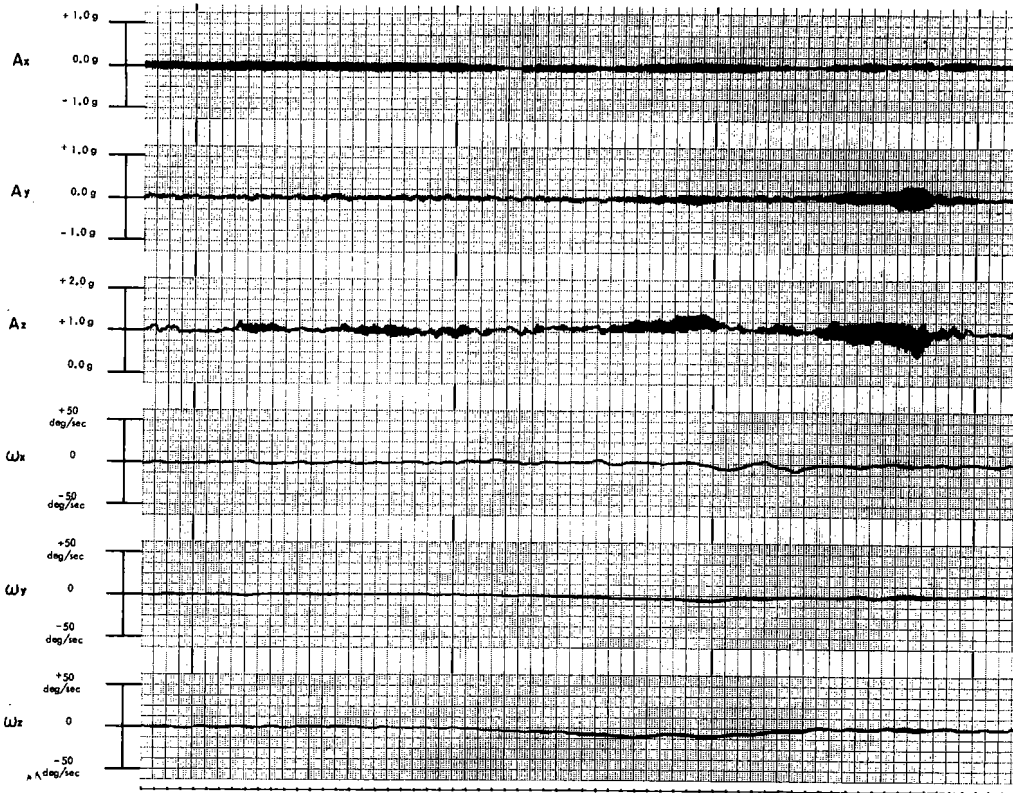


Figure 39. CH-54 "Flying Crane" flight data collected during a typical landing approach made from a right turn: 0 to 5 cps filter.

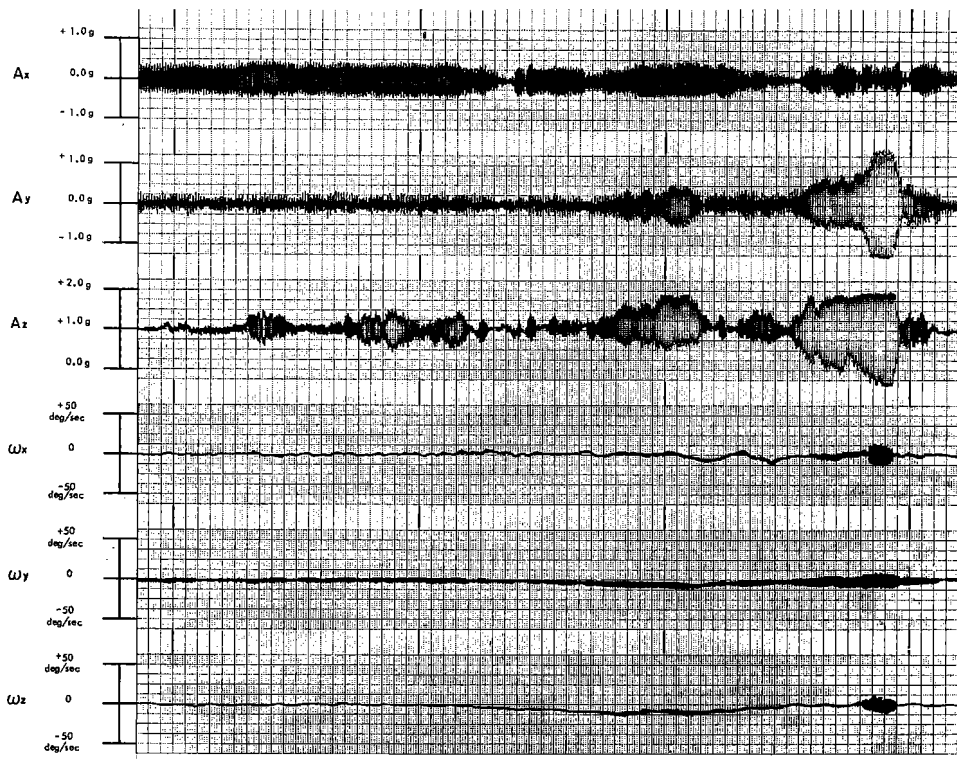


Figure 40. CH-54 flight data: Same as Figure 39 except not filtered.

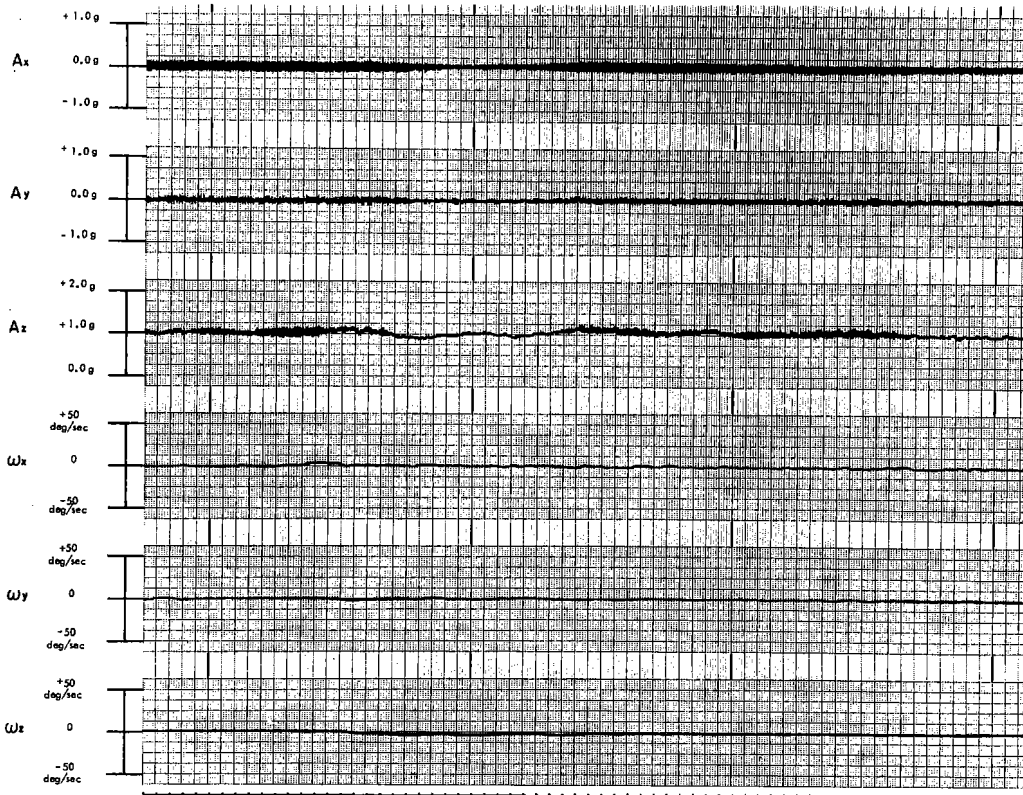


Figure 41. CH-54 flight data collected during an 80-knot descending right turn: 0 to 5 cps filter.

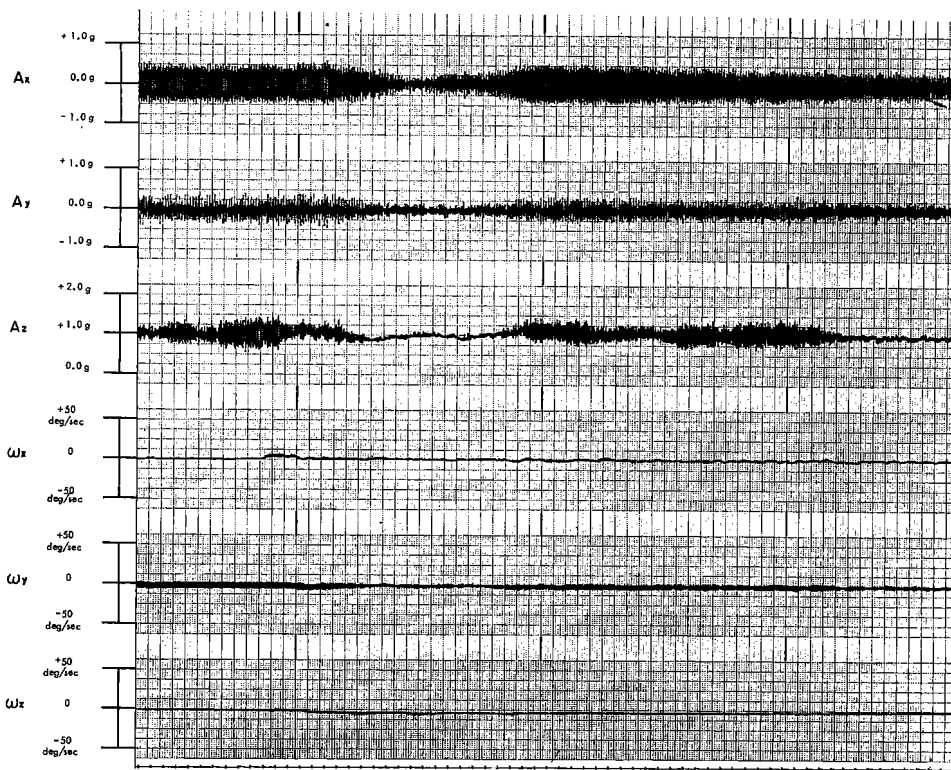


Figure 42. CH-54 flight data: Same as Figure 41 except not filtered.

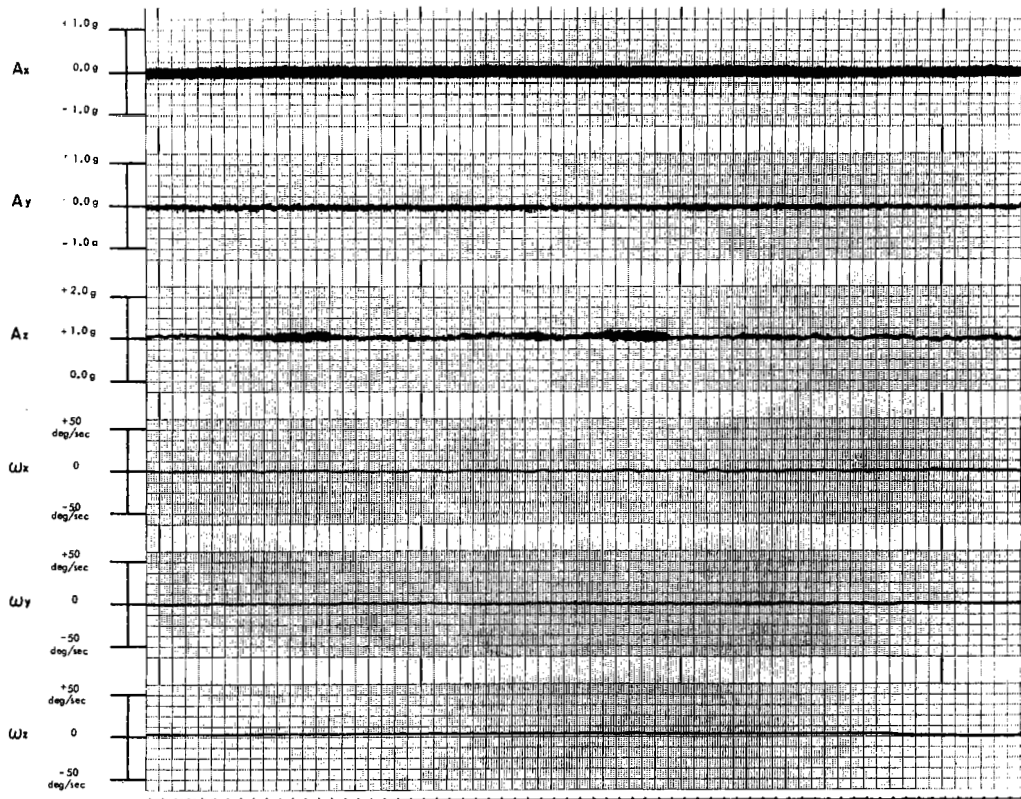


Figure 43. CH-54 flight data collected during an 80-knot gradual left turn: 0 to 5 cps filter.

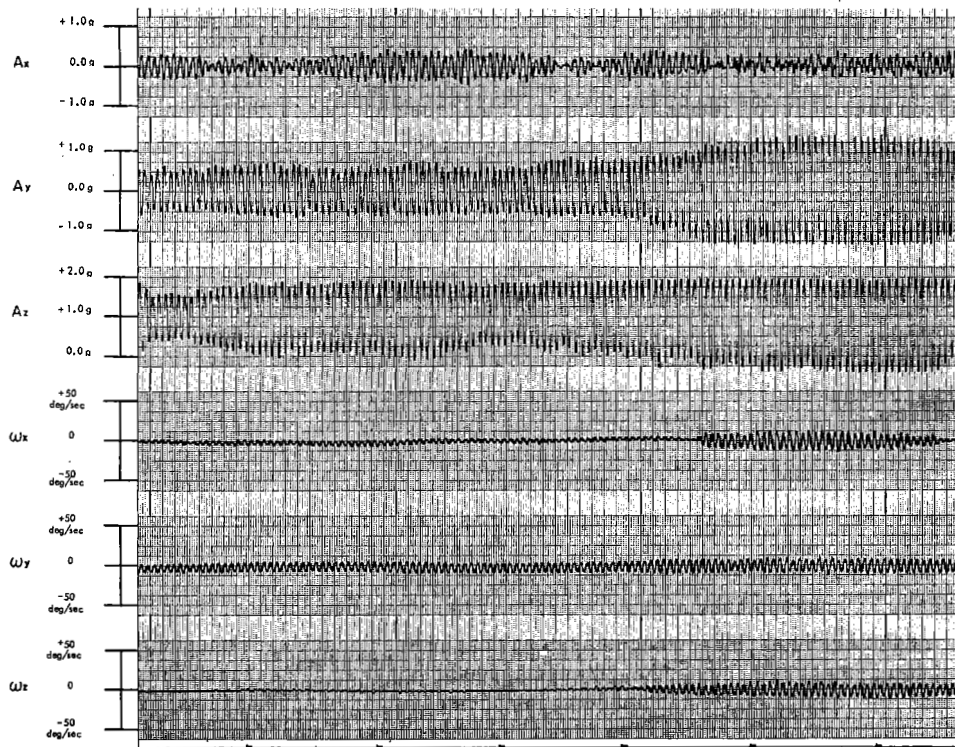


Figure 44. CH-54 flight data: Expanded time-base recording made during a landing approach. Data not filtered.

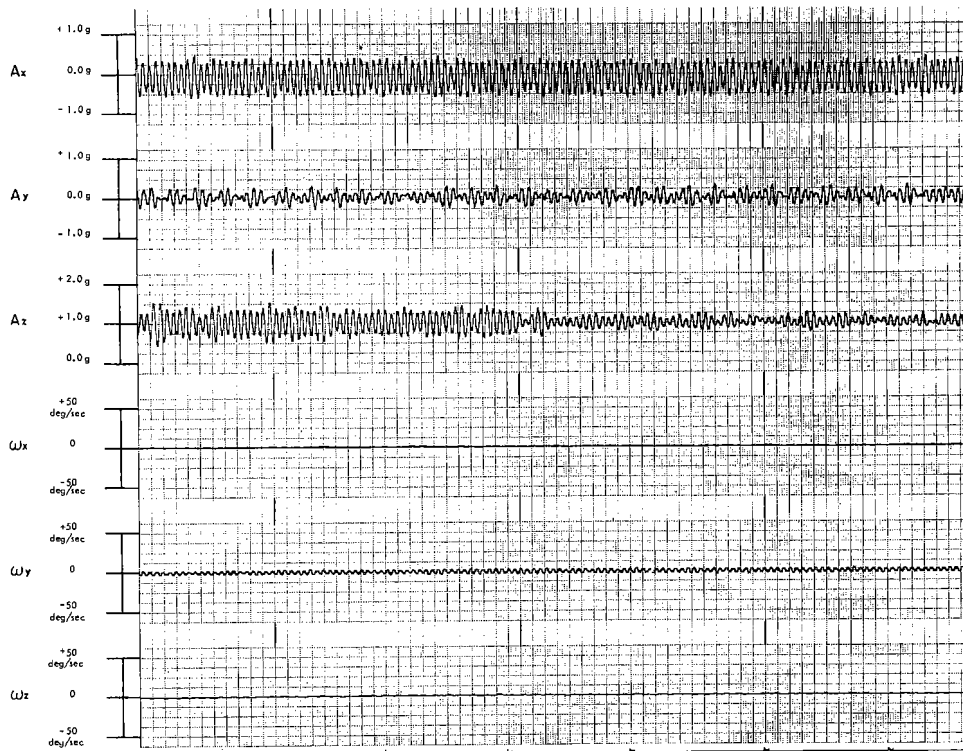


Figure 45. CH-54 flight data: Expanded time-base recording made during straight and level flight at 80 knots. Data not filtered.

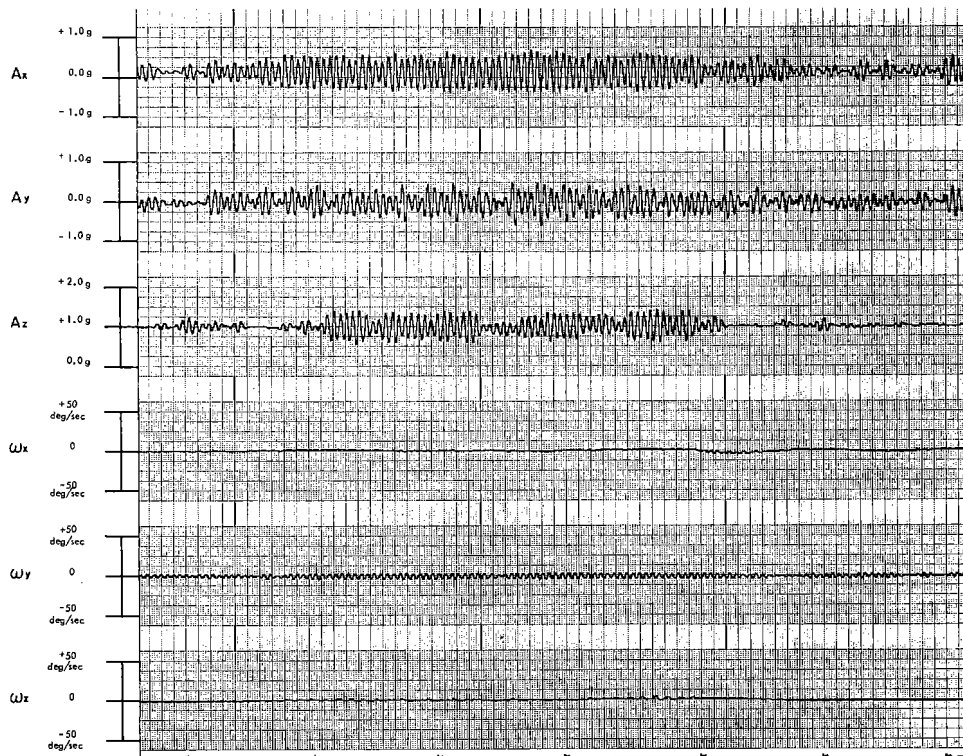


Figure 46. CH-54 flight data: Expanded time-base recording made while hovering. Data not filtered.

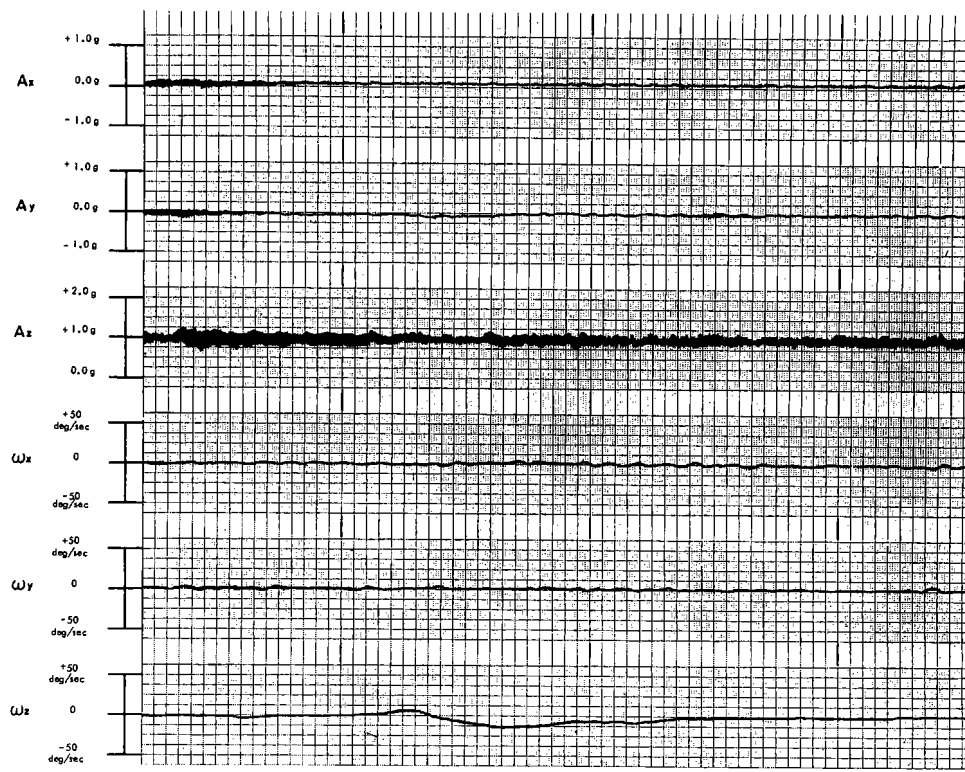


Figure 47. CH-47A "Chinook" flight data collected during a landing approach: 0 to 5 cps filter.

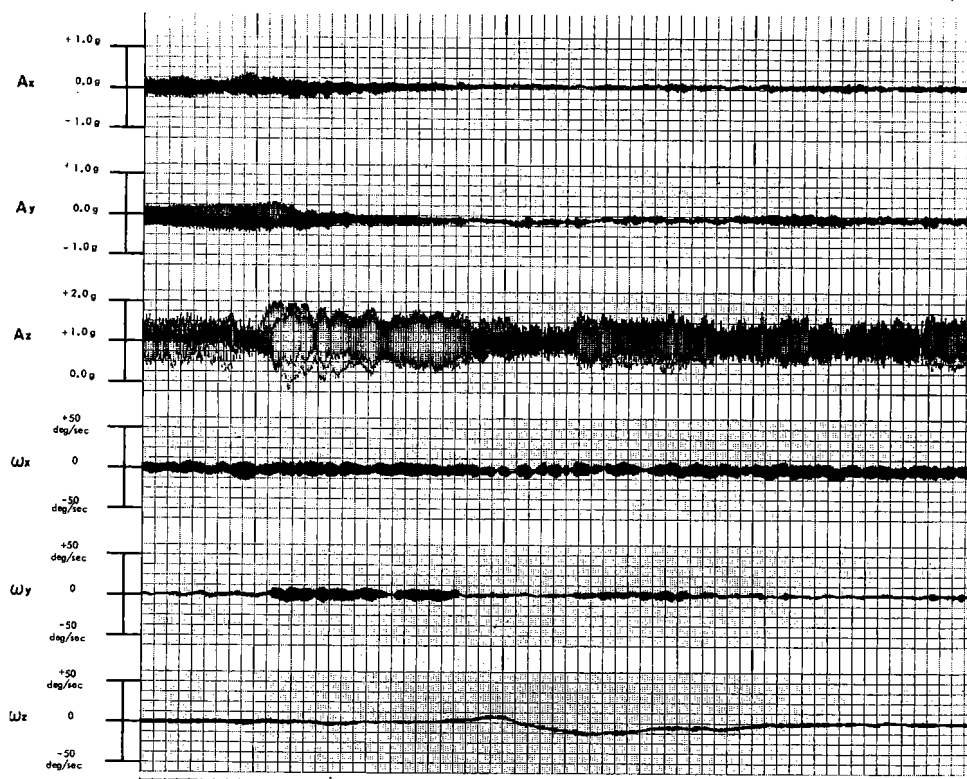


Figure 48. CH-47A flight data: Same as Figure 47 except not filtered.

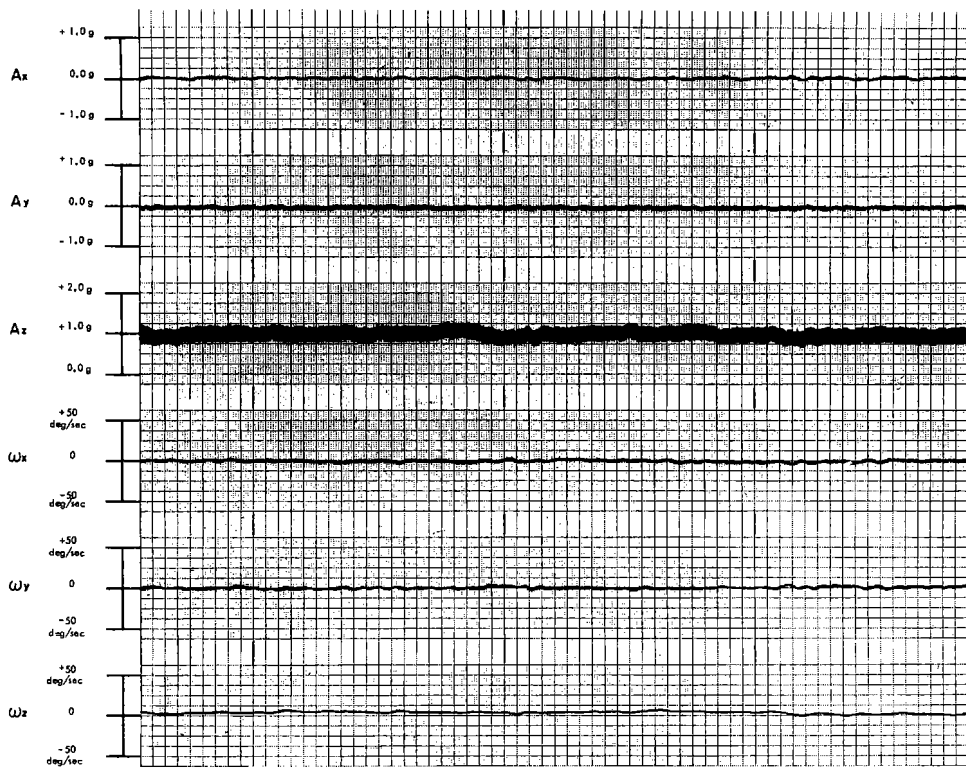


Figure 49. CH-47A flight data collected during a left turn with a swing load: 0 to 5 cps filter.

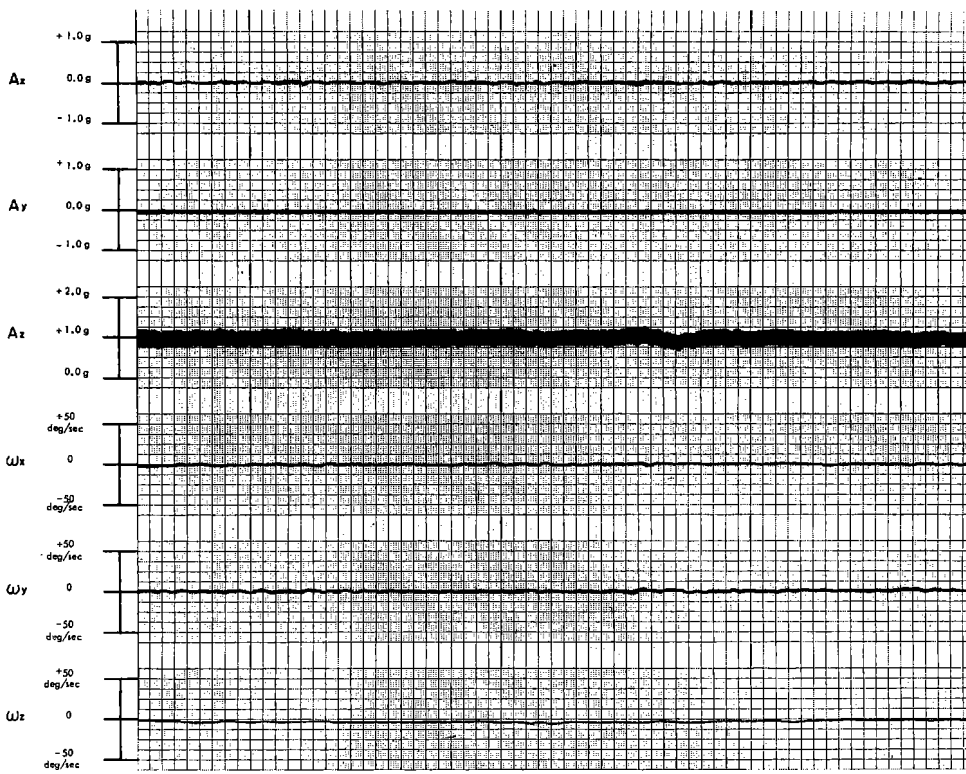


Figure 50. CH-47A flight data collected during a right turn with a swing load: 0 to 5 cps filter.

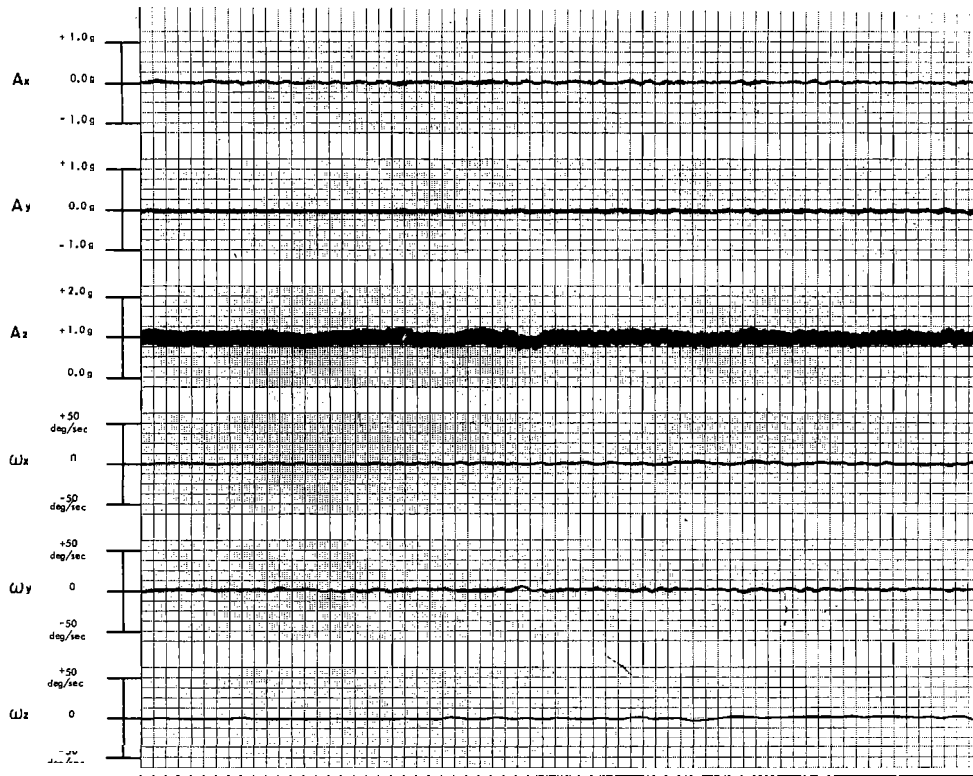


Figure 51. CH-47A flight data collected during straight and level flight at 100 knots: 0 to 5 cps filter.

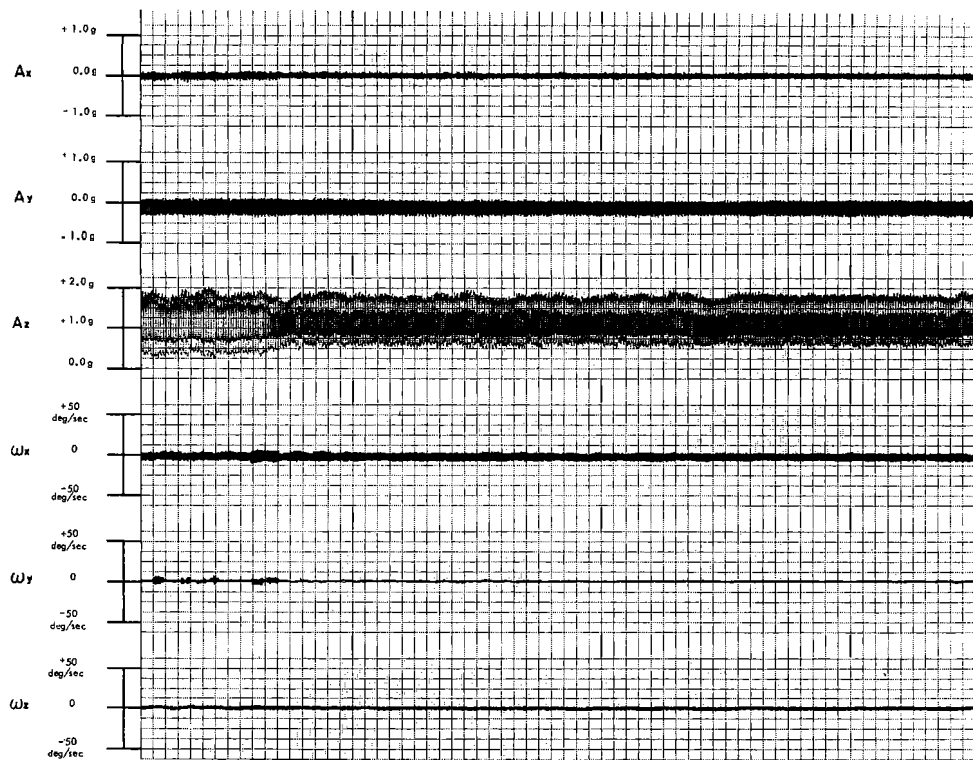


Figure 52. CH-47A flight data: Same as Figure 51 except not filtered.

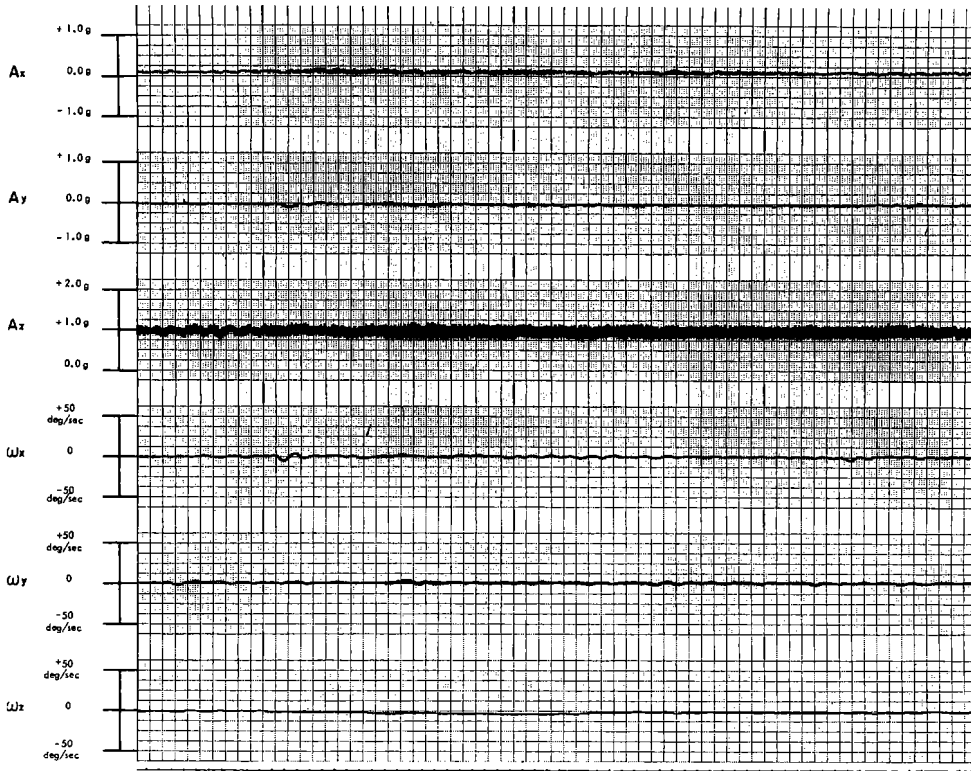


Figure 53. CH-47A flight data collected in typical hover with swing load: 0 to 5 cps filter.

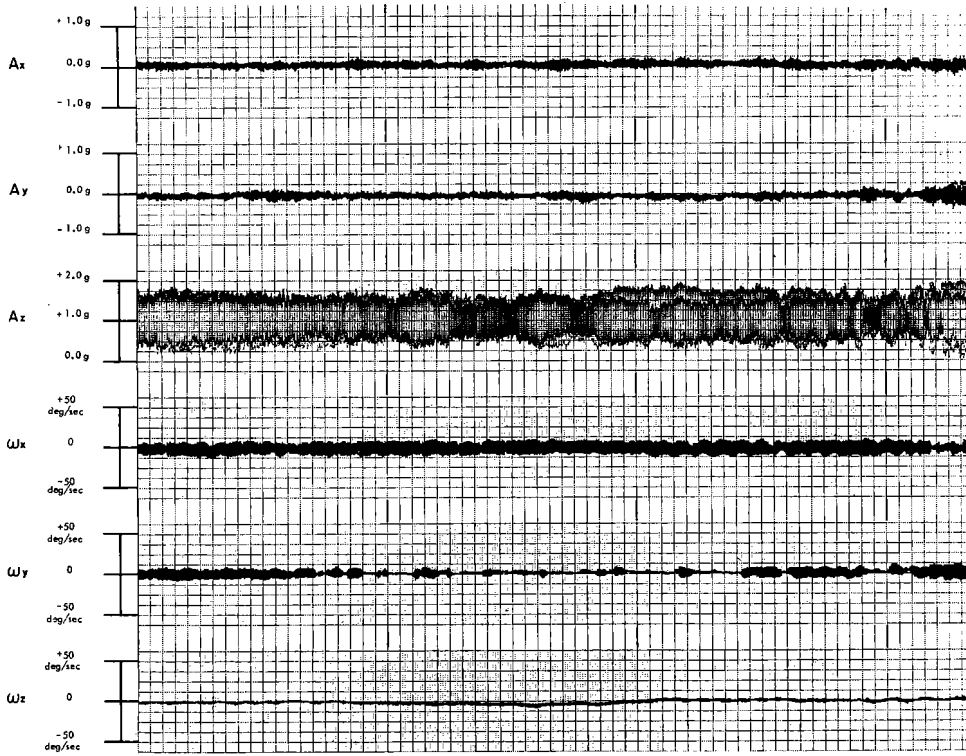


Figure 54. CH-47A flight data: Same as Figure 53 except not filtered.

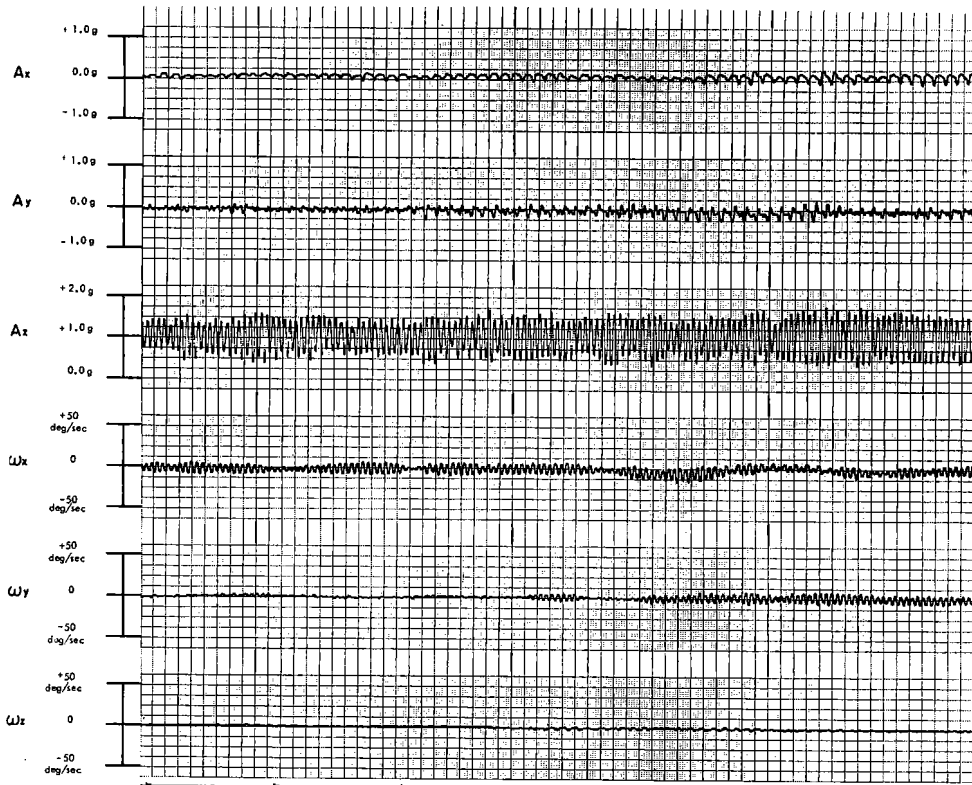


Figure 55. CH-47A flight data: Expanded time-base recording made during a typical hover with swing load. Data not filtered.

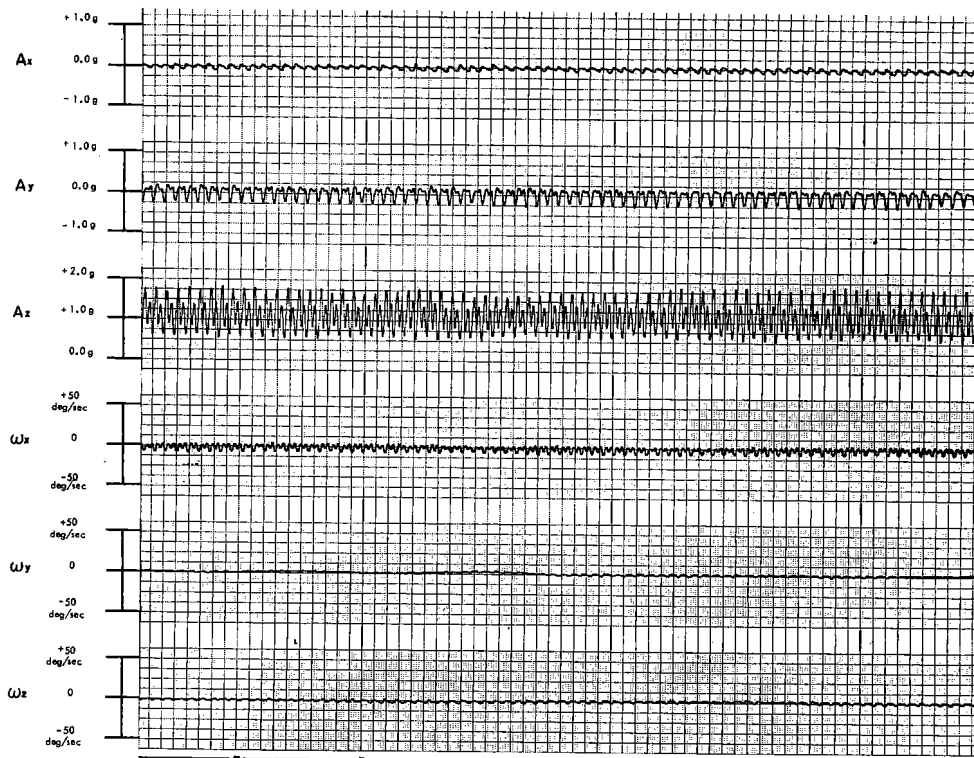


Figure 56. CH-47A flight data: Expanded time-base recording made during straight and level flight at 100 knots. Data not filtered.

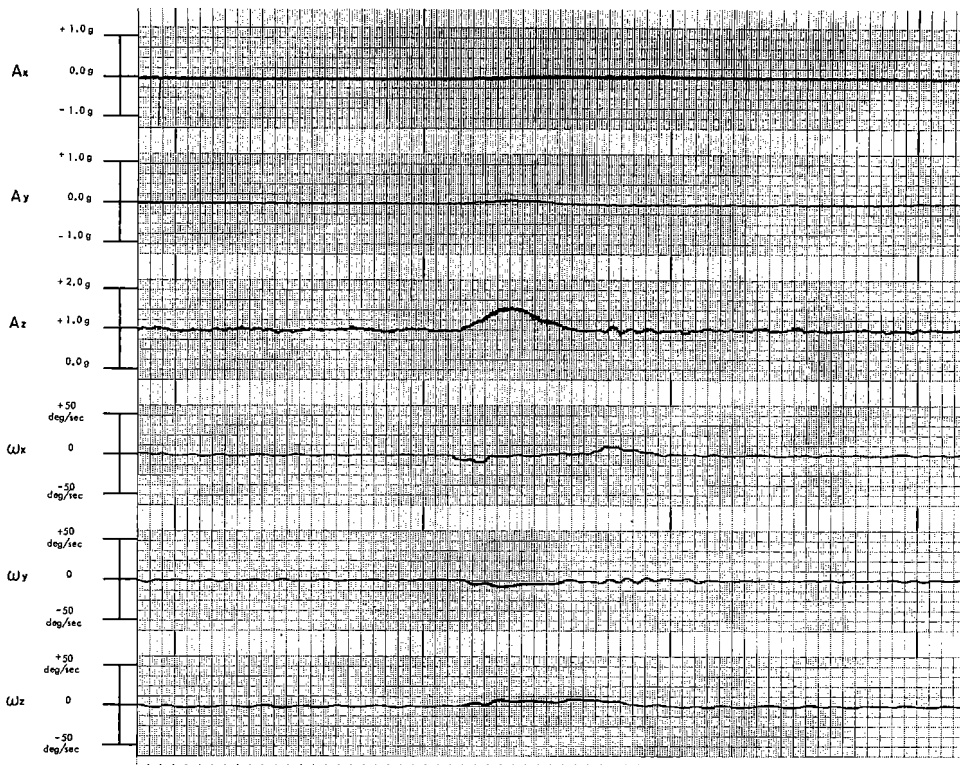


Figure 57. UH-2B "Seasprite" flight data collected during a 90-knot climbing left turn: 0 to 5 cps filter.

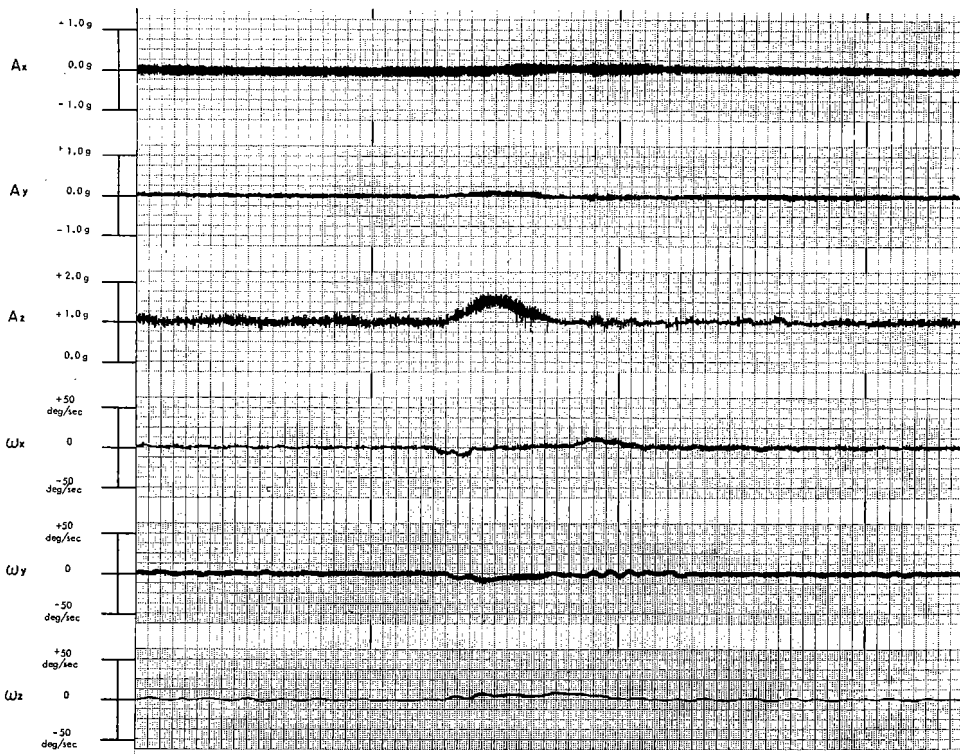


Figure 58. UH-2B flight data: Same as Figure 57 except not filtered.

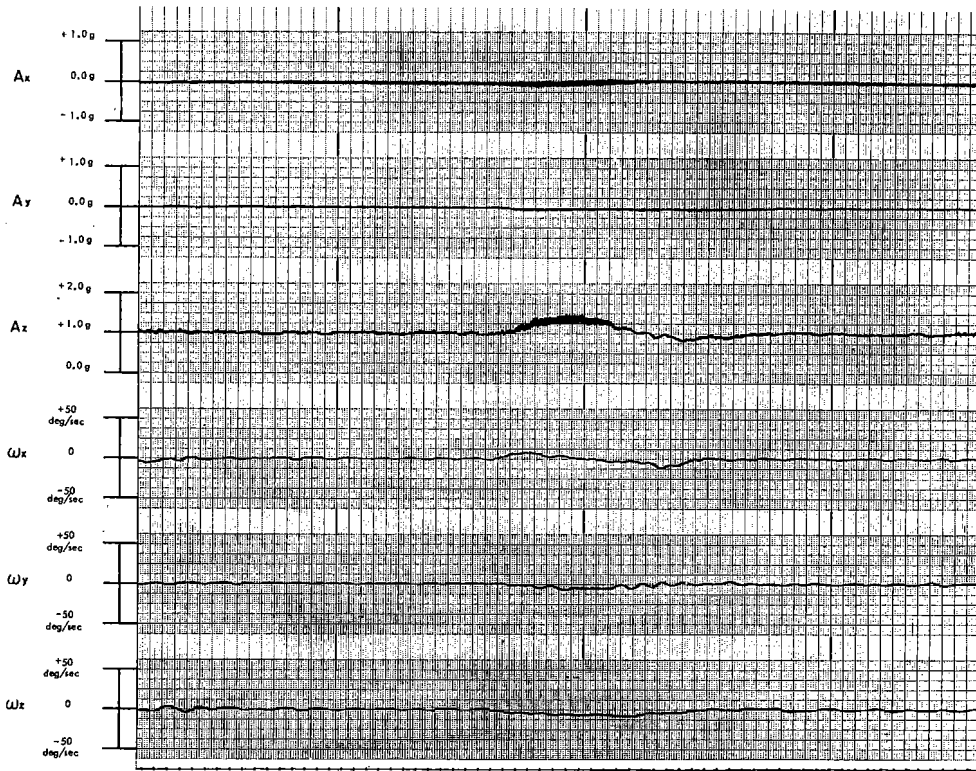


Figure 59. UH-2B flight data collected during a 90-knot climbing right turn: 0 to 5 cps filter.

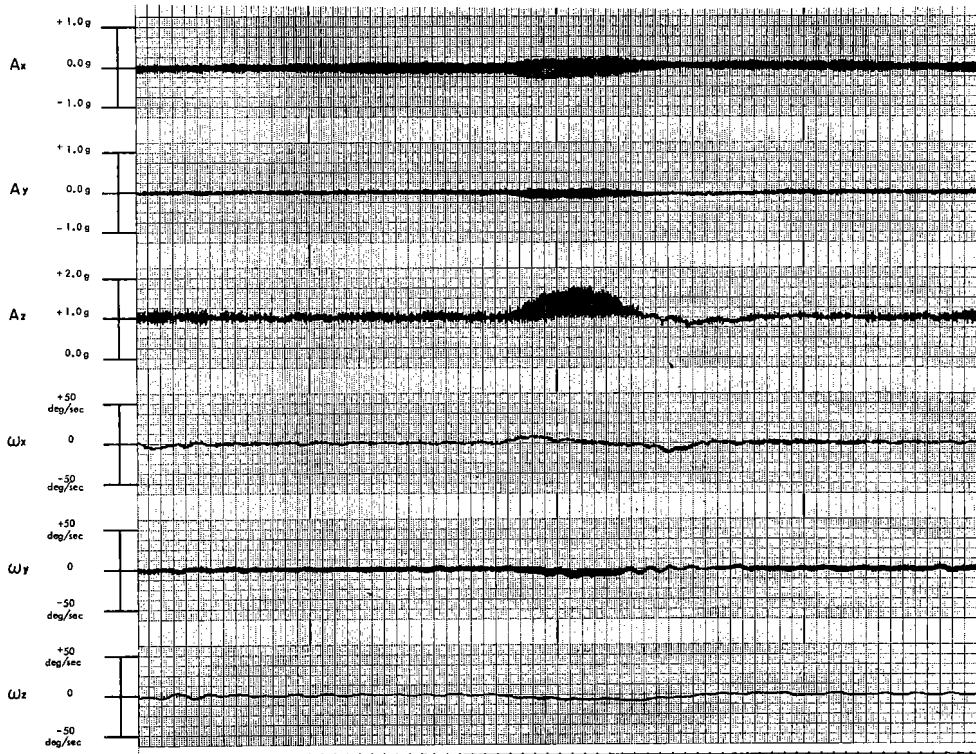


Figure 60. UH-2B flight data: Same as Figure 59 except not filtered.

Figure 62. UH-2B flight data: Expanded time-base recording made during liftoff. Data not filtered.

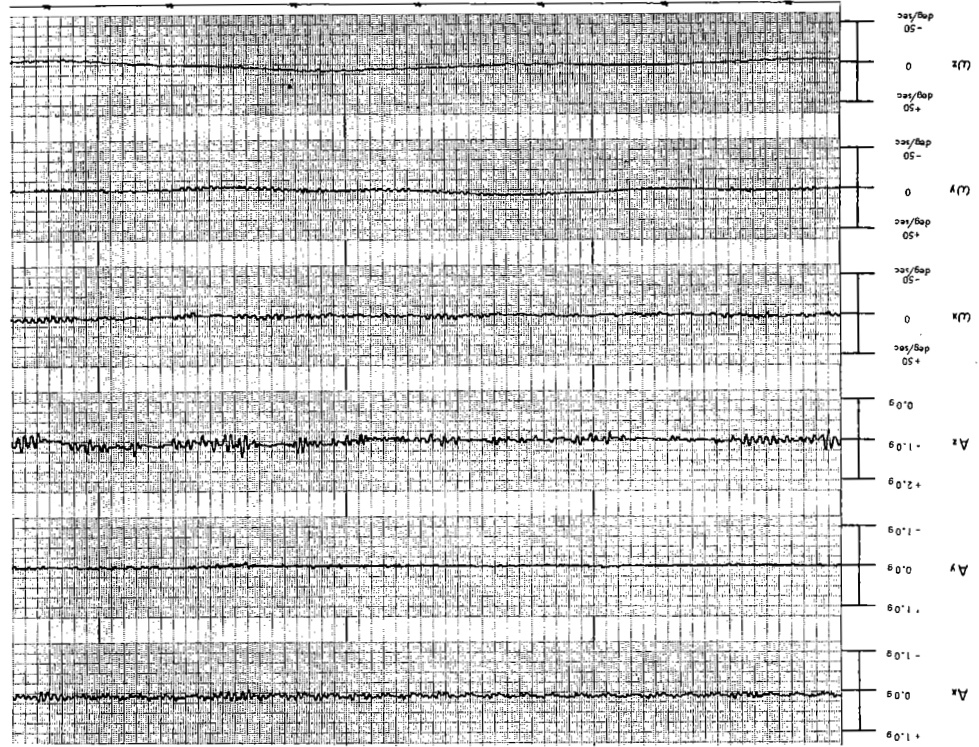
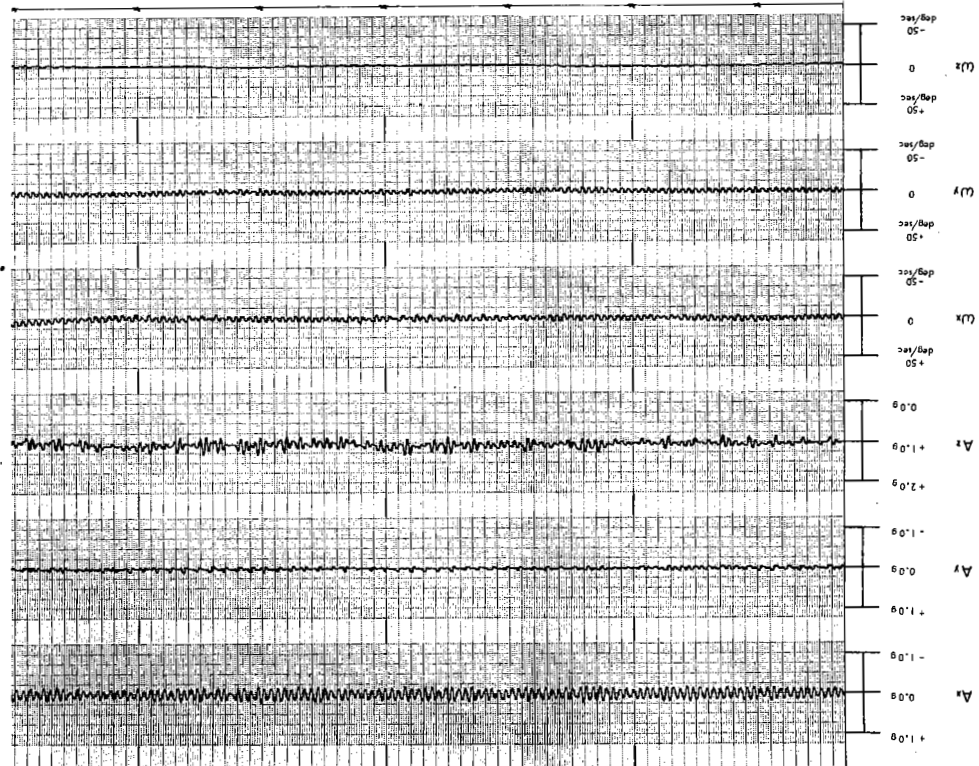


Figure 61. UH-2B flight data: Expanded time-base recording made during straight and level flight at 90 knots. Data not filtered.



Unclassified

Security Classification

DOCUMENT CONTROL DATA - R & D

(Security classification of title, body of abstract and indexing annotation must be entered when the overall report is classified)

|   |  |   |                      |
|---|--|---|----------------------|
| 1. ORIGINATING ACTIVITY (Corporate author)<br>Naval Aerospace Medical Institute<br>Pensacola, Florida 32512   |  | 2a. REPORT SECURITY CLASSIFICATION<br>Unclassified  |                      |
|   |  | 2b. GROUP<br>N/A  |                      |
| 3. REPORT TITLE<br><br>SAMPLE HELICOPTER FLIGHT MOTION DATA FOR VESTIBULAR REFERENCE  |  |   |                      |
| 4. DESCRIPTIVE NOTES (Type of report and inclusive dates)   |  |   |                      |
| 5. AUTHOR(S) (First name, middle initial, last name)<br><br>W. Carroll Hixson and Jorma I. Niven  |  |   |                      |
| 6. REPORT DATE<br>2 November 1969   |  | 7a. TOTAL NO. OF PAGES<br>39  | 7b. NO. OF REFS<br>3 |
| 8a. CONTRACT OR GRANT NO.   |  | 9a. ORIGINATOR'S REPORT NUMBER(S)<br><br>NAMI-1094  |                      |
| b. PROJECT NO.<br>MF12.524.005-5016B  |  | 9b. OTHER REPORT NO(S) (Any other numbers that may be assigned this report)<br><br>3 and USAARL Serial No. 70-7 |                      |
| c.  |  |   |                      |
| d.  |  |   |                      |
| 10. DISTRIBUTION STATEMENT<br><br>This document has been approved for public release and sale; its distribution is unlimited.   |  |   |                      |
| 11. SUPPLEMENTARY NOTES<br><br>Joint report with U.S. Army Aeromedical Research Laboratory, Fort Rucker, Alabama  |  | 12. SPONSORING MILITARY ACTIVITY  |                      |
| 13. ABSTRACT<br><br>This report presents low-frequency linear and angular motion flight data collected on a noninterference basis aboard the following military helicopters: AH-1G, UH-1B, UH-1D, OH-6A, CH-54, CH-47, and UH-2B. Measurement data recorded during various tactical maneuvers and routine flight operations included the triaxial linear accelerations occurring along the roll, pitch, and yaw axes and the triaxial angular velocities occurring about the same three reference axes. |  |   |                      |

Unclassified

Security Classification

| 14. KEY WORDS        | LINK A |    | LINK B |    | LINK C |    |
|----------------------|--------|----|--------|----|--------|----|
|                      | ROLE   | WT | ROLE   | WT | ROLE   | WT |
| Instrumentation      |        |    |        |    |        |    |
| Helicopters          |        |    |        |    |        |    |
| Linear acceleration  |        |    |        |    |        |    |
| Angular velocity     |        |    |        |    |        |    |
| Vestibular system    |        |    |        |    |        |    |
| Pilot disorientation |        |    |        |    |        |    |

Unclassified

Security Classification